2

Adaptive Backstepping Flight Control for Modern Fighter Aircraft

L. Sonneveldt, Q.P. Chu and J.A. Mulder
Delft University of Technology
The Netherlands

1. Introduction

Inertial trajectory control is essential for UAVs which must follow predetermined paths through three-dimensional space (Healy and Liebard, 1993, Kaminer et al., 1998, Boyle et al., 1999, Singh et al., 2003, Tsach et al., 2003, Ren and Beard, 2004, Wegener et al., 2004, Ren and Atkins, 2005, No et al., 2005, Clough, 2005, Papadales et al., 2005, Narasimhan et al., 2006, Kaminer et al., 2007). Other applications of trajectory control include formation flight, aerial refueling, and autonomous landing maneuvers (Pachter et al., 1994, Proud et al., 1999, Fujimori et al. 2000, Singh et al., 2000, Pachter et al., 2001, Wang et al., 2008).

Two different approaches can be distinguished in the design of these trajectory control systems. The most popular approach is to separate the guidance and control laws: a given reference trajectory is converted by the guidance laws to velocity and attitude commands for the autopilot, which in turn generates the actuator signals (Ren and Beard, 2004, Pachter et al., 1994, Pachter et al., 2001). Usually, the assumption is made that the autopilot response to heading and airspeed commands is first order in nature to simplify the design.

The other design approach is to integrate the guidance and control laws into one system, in order to achieve better stability guarantees and improved performance. Kaminer et al. (1998) use an integrated guidance and control approach to trajectory tracking in which the trimmed flight conditions along the reference trajectory are the command input to the tracking controllers. Singh (2003) uses a combination of sliding-mode control and adaptive control.

In this chapter an integrated, though cascaded Lyapunov-based adaptive backstepping (Krstić et al., 1992, Singh and Steinberg 1996) approach is taken and used to design a flight-path controller for a nonlinear high-fidelity F-16 model. Adaptive backstepping allows assuming that the aerodynamic force and moment models may not be known exactly, and even that they may change in flight due to causes as structural damage and control actuator failures. There is much literature available on adaptive backstepping control system design for aircraft and missiles (see, for example, (Singh and Steinberg, 1996, Härkegård, 2003, Farrell et al., Kim et al., 2004, Shin and Kim, 2004, Farrell et al., 2005, Sonneveldt, et al., 2006, Sonneveldt, et al. 2007)). Most of these designs consider control of the aerodynamic angles μ, a, and β. Due to the higher relative degree, however, the design of trajectory controllers as discussed here is much more complicated, as the required analytical calculation of the derivatives of the intermediate control variables leads to a rapid explosion of terms. This phenomenon is the main motivation for the authors of (Singh et al., 2003) to select a sliding-

mode design for the outer feedback loops. Another disadvantage of (adaptive) backstepping flight control system design is that the contribution of the control-surface deflections to the aerodynamic forces cannot be taken into account. For these reasons, the constrained adaptive backstepping approach of (Farrell et al., 2005, Sonneveldt et al., 2007, Yip 1997) is used here. This method makes use of command filters to calculate the derivatives of the intermediate controls, which greatly simplifies the design. Additionally, these filters can be used to enforce magnitude and rate limits on the state and input variables.
To simplify the mathematical approximation of the unknown aerodynamic force and moment characteristics, we propose to partition the flight envelope into multiple connecting operating regions called hyperboxes. In each hyperbox a locally valid linear-in-the-parameters nonlinear model is defined. The coefficients of these local models can be estimated using the update laws of the adaptive backstepping control laws. The number and size of the hyperboxes should be based on a priori information on the physical properties of the vehicle on hand, and may be defined in terms of state variables as Mach number, angle of attack and engine thrust. In this study we use B-spline neural networks (Cheng et al., 1999, Ward et al., 2003) to interpolate between the local models to ensure smooth model transitions. Numerical simulations of various maneuvers with aerodynamic uncertainties in the model and actuator failures are presented. The maneuvers are performed at several flight conditions to demonstrate that the control laws are valid for the entire flight envelope.
The chapter is outlined as follows. First, the nonlinear dynamics of the aircraft model are introduced in Sec. II. In Sec. III the adaptive control system design is presented decomposed in four cascaded feedback-loop designs. The aerodynamic model identification process including the B-spline neural networks is discussed in Sec. IV. Section V validates the performance of the control laws using numerical simulations performed in MATLAB/Simulink. A summary of the results and the conclusions are given in Sec. VI. Finally, an appendix on the concept of constrained adaptive backstepping is included.

2. Aircraft model description

The aircraft model used in this study is that of an F-16 fighter aircraft with geometry and aerodynamic data as reported in (Nguyen et al., 1979). The aerodynamic data in tabular form have been obtained from wind-tunnel tests and are valid up to Mach 0.6 for the wide range of -20 deg $\leq \alpha \leq$ 90 deg and -30 deg $\leq \beta \leq$ 30 deg. The control inputs of the model are the elevator, ailerons, rudder, and leading-edge flaps, as well as the throttle setting. The leading-edge flaps are not used in the control design. The control-surface actuators are modeled as first-order low-pass filters with rate and magnitude limits as given in (Sonneveldt et al., 2007). Before giving the equations of motion for the F-16 model, some reference frames to describe the aircraft motion are needed. The reference frames used in this paper are the Earth-fixed reference frame F_E, used as the inertial frame; the vehicle-carried local Earth reference frame F_O, with its origin fixed in the center of gravity of the aircraft, which is assumed to have the same orientation as F_E; the wind-axes reference frame F_W, obtained from F_O by three successive rotations of χ, γ, and μ; the stability-axes reference frame F_S, obtained from F_W by a rotation of $-\beta$; and the body-fixed reference frame F_B, obtained from F_S by a rotation of α, as is also indicated in Fig. 1. The body-fixed reference frame F_B can also be obtained directly from F_O by three successive rotations of yaw angle ψ, pitch angle θ, and roll angle ϕ. More details and transformation matrices are given in, for example, (Lewis and Stevens, 1992, Cook, 1997).

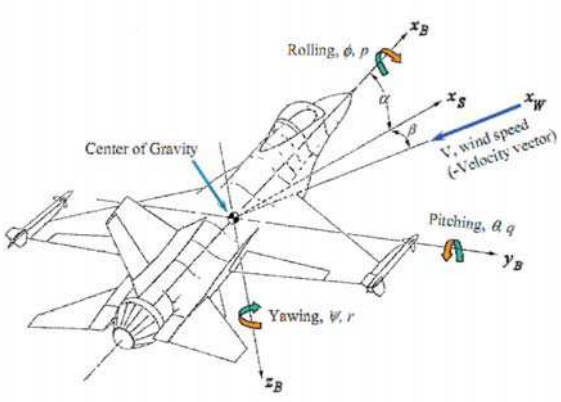

Fig. 1. Aircraft reference frames

Assuming that the aircraft has a rigid body, which is symmetric around the X–Z body-fixed plane, the relevant nonlinear coupled equations of motion can be described by (Lewis and Stevens, 1992):

$$\dot{X}_0 = \begin{bmatrix} V\cos\chi\cos\gamma \\ V\sin\chi\cos\gamma \\ -V\sin\gamma \end{bmatrix} \tag{1}$$

$$\dot{X}_1 = \begin{bmatrix} \frac{1}{m}\left(-D + T\cos\alpha\cos\beta\right) - g\sin\gamma \\ \frac{1}{mV\cos\gamma}\left[L\sin\mu + Y\cos\mu + T\left(\sin\alpha\sin\mu - \cos\alpha\sin\beta\cos\mu\right)\right] \\ \frac{1}{mV}\left[L\cos\mu - Y\sin\mu + T\left(\cos\alpha\sin\beta\sin\mu + \sin\alpha\cos\mu\right)\right] - \frac{g}{V}\cos\gamma \end{bmatrix} \tag{2}$$

$$\dot{X}_2 = \begin{bmatrix} \frac{\cos\alpha}{\cos\beta} & 0 & \frac{\sin\alpha}{\cos\beta} \\ -\cos\alpha\tan\beta & 1 & -\sin\alpha\tan\beta \\ \sin\alpha & 0 & -\cos\alpha \end{bmatrix} X_3 + \begin{bmatrix} 0 & \sin\gamma + \cos\gamma\sin\mu\tan\beta & \cos\mu\tan\beta \\ 0 & -\frac{\cos\gamma\sin\mu}{\cos\beta} & -\frac{\cos\mu}{\cos\beta} \\ 0 & \cos\gamma\cos\mu & -\sin\mu \end{bmatrix} \dot{X}_1 \tag{3}$$

$$\dot{X}_3 = \begin{bmatrix} \left(c_1 r + c_2 p\right)q + c_3\bar{L} + c_4\left(\bar{N} + h_e q\right) \\ c_5 pr - c_6\left(p^2 - r^2\right) + c_7\left(\bar{M} - h_e r\right) \\ \left(c_8 p - c_2 r\right)q + c_4\bar{L} + c_9\left(\bar{N} + h_e q\right) \end{bmatrix} \tag{4}$$

where $X_0 = \begin{bmatrix} x & y & z \end{bmatrix}^T$, $X_1 = \begin{bmatrix} V & \chi & \gamma \end{bmatrix}^T$, $X_2 = \begin{bmatrix} \mu & \alpha & \beta \end{bmatrix}^T$, $X_3 = \begin{bmatrix} p & q & r \end{bmatrix}^T$, and the definition of the inertia terms $c_i\left(i = 1, \cdots, 9\right)$ is given in, for example, (Sonneveldt et al., 2007).

The engine angular momentum h_e is assumed to be constant. These 12 differential equations are sufficient to describe the complete motion of the aircraft; other states such as the attitude angles ϕ, θ, and ψ are functions of X_3, and their dynamics can be expressed as

$$\begin{bmatrix} \dot{\phi} \\ \dot{\theta} \\ \dot{\psi} \end{bmatrix} = \begin{bmatrix} 1 & \sin\phi\tan\theta & \cos\phi\tan\theta \\ 0 & \cos\phi & -\sin\phi \\ 0 & \dfrac{\sin\phi}{\cos\theta} & \dfrac{\cos\phi}{\cos\theta} \end{bmatrix} X_3 \tag{5}$$

The thrust model of (Nguyen et al., 1979) is implemented, which calculates the thrust as a function of altitude, Mach number, and throttle setting δ_t. This model is given in tabular form. The aerodynamic forces *L*, *Y*, and *D* (expressed in the wind reference frame F_W) and moments $\bar{L}$, $\bar{M}$, and $\bar{N}$ (expressed in body fixed frame F_B) are summations of the various aerodynamic contributions stored in lookup tables. As an example, the pitch moment $\bar{M}$ is given by

$$\begin{aligned} \bar{M} = \bar{q}S\bar{c}\Bigg\{ & C_m(\alpha,\beta,\delta_e) + C_{Z_T}\cdot\left(x_{cg_r} - x_{cg}\right) + \delta C_{m_{LEF}}\left(1 - \frac{\delta_{LEF}}{25}\right) + \\ & + \frac{q\bar{c}}{2V_T}\left(C_{m_q}(\alpha) + \delta C_{m_{qLEF}}(\alpha)\right)\left(1 - \frac{\delta_{LEF}}{25}\right) + \delta C_m(\alpha) + \delta C_{m_{ds}}(\alpha,\delta_e)\Bigg\} \end{aligned} \tag{6}$$

Other aerodynamic forces and moments are given in similar form; for a detailed discussion, see (Nguyen et al., 1979).

3. Adaptive control design

In this section we aim to develop an adaptive guidance and control system that asymptotically tracks a smooth prescribed inertial trajectory $Y^{\text{ref}} = \begin{pmatrix} x^{\text{ref}} & y^{\text{ref}} & z^{\text{ref}} \end{pmatrix}^T$ with position states $X_0 = \begin{pmatrix} x & y & z \end{pmatrix}^T$. Furthermore, the sideslip angle β has to be kept at zero to enable coordinated turning. It is assumed that the reference trajectory $Y^{\text{ref}} = \begin{pmatrix} x^{\text{ref}} & y^{\text{ref}} & z^{\text{ref}} \end{pmatrix}^T$ satisfies

$$\dot{x}^{\text{ref}} = V^{\text{ref}}\cos\chi^{\text{ref}} \tag{7}$$

$$\dot{y}^{\text{ref}} = V^{\text{ref}}\sin\chi^{\text{ref}} \tag{8}$$

with V^{ref}, χ^{ref}, z^{ref}, and their derivatives continuous and bounded. It also assumed that the components of the total aerodynamic forces *L*, *Y*, and *D* and moments $\bar{L}$, $\bar{M}$ and $\bar{N}$ are uncertain, and so these will have to be estimated. The available controls are the control-surface deflections $\begin{pmatrix} \delta_e & \delta_a & \delta_r \end{pmatrix}^T$ and the engine thrust *T*. The Lyapunov-based control design based on (Farrell et al., 2005, Sonneveldt et al., 2007) is done in four feedback loops, starting at the outer loop.

3.1 Inertial position control

We start the outer-loop feedback control design by transforming the tracking control problem into a regulation problem:

$$Z_0 = \begin{bmatrix} z_{01} \\ z_{02} \\ z_{03} \end{bmatrix} = \begin{bmatrix} \cos\chi & \sin\chi & 0 \\ -\sin\chi & \cos\chi & 0 \\ 0 & 0 & 1 \end{bmatrix} \left(X_0 - Y^{\text{ref}} \right) \tag{9}$$

where we introduce a vehicle carried vertical reference frame with origin in the center of gravity and X-axis aligned with the horizontal component of the velocity vector (Ren and Beard, 2004, Proud et al., 1999). Differentiating Eq. (9) now gives

$$\dot{Z}_0 = \begin{bmatrix} V + z_{02}\dot{\chi} - V^{\text{ref}} \cos\left(\chi - \chi^{\text{ref}}\right) \\ -z_{01}\dot{\chi} + V^{\text{ref}} \sin\left(\chi - \chi^{\text{ref}}\right) \\ \dot{z}^{\text{ref}} - V\sin\gamma \end{bmatrix} \tag{10}$$

We want to control the position errors Z_0 through the flight-path angles χ and γ, and the total airspeed V. However, from Eq. (10) it is clear that it is not yet possible to do something about z_{02} in this design step. Now we select the virtual controls

$$V^{\text{des},0} = V^{\text{ref}} \cos\left(\chi - \chi^{\text{ref}}\right) - c_{01} z_{01} \tag{11}$$

$$\gamma^{\text{des},0} = \arcsin\left(\frac{c_{03} z_{03} - \dot{z}^{\text{ref}}}{V} \right), \quad -\frac{\pi}{2} < \gamma < \frac{\pi}{2} \tag{12}$$

where $c_{01} > 0$ and $c_{03} > 0$ are the control gains. The actual implementable virtual control signals V^{des} and γ^{des}, as well as their derivatives, $\dot{V}^{\text{des}}$ and $\dot{\gamma}^{\text{des}}$, are obtained by filtering the virtual signals with a second-order low-pass filter. In this way, tedious calculation of the virtual control derivatives is avoided (Swaroop et al., 1997). An additional advantage is that the filters can be used to enforce magnitude or rate limits on the states (Farrell et al., 2003, 2007). As an example, the state-space representation of such a filter for $V^{\text{des},0}$ is given by

$$\begin{bmatrix} \dot{q}_1(t) \\ \dot{q}_2(t) \end{bmatrix} = \begin{bmatrix} q_2 \\ 2\zeta_V \omega_V \left(S_R\left(\frac{\omega_V^2}{2\zeta_V \omega_V} \left[S_M\left(V^{\text{des},0} \right) - q_1 \right] \right) - q_2 \right) \end{bmatrix} \tag{13}$$

$$\begin{bmatrix} V^{\text{des}} \\ \dot{V}^{\text{des}} \end{bmatrix} = \begin{bmatrix} q_1 \\ q_2 \end{bmatrix} \tag{14}$$

where $S_M(\cdot)$ and $S_R(\cdot)$ represent the magnitude and rate limit functions as given in (Farrell et al., 2007). These functions enforce the state V to stay within the defined limits. Note that if

the signal $V^{\mathrm{des},0}$ is bounded, then V^{des} and $\dot{V}^{\mathrm{des}}$ are also bounded and continuous signals. When the magnitude and rate limits are not in effect, the transfer function from $V^{\mathrm{des},0}$ to V^{des} is given by

$$\frac{V^{\mathrm{des}}}{V^{\mathrm{des},0}} = \frac{\omega_V^2}{s^2 + 2\zeta_V \omega_V + \omega_V^2} \tag{15}$$

and the error $V^{\mathrm{des},0} - V^{\mathrm{des}}$ can be made arbitrarily small by selecting the bandwidth of the filter to be sufficiently large (Swaroop et al., 1997).

3.2 Flight-path angle and airspeed control

In this loop the objective is to steer V and γ to their desired values, as determined in the previous section. Furthermore, the heading angle χ has to track the reference signal χ^{ref}, and we also have to guarantee that z_{02} is regulated to zero. The available (virtual) controls in this step are the aerodynamic angles μ and α, as well as the thrust T. The lift, drag, and side forces are assumed to be unknown and will be estimated. Note that the aerodynamic forces also depend on the control-surface deflections $U = \begin{bmatrix} \delta_e & \delta_a & \delta_r \end{bmatrix}^T$. These forces are quite small, because the surfaces are primarily moment generators. However, because the current control-surface deflections are available from the command filters used in the inner loop, we can still take them into account in the control design. The relevant equations of motion are given by

$$\dot{X}_1 = A_1 F_1(X,U) + B_1 G_1(X,U,X_2) + H_1(X) \tag{16}$$

where

$$A_1 = \frac{1}{mV}\begin{bmatrix} 0 & 0 & -V \\ 0 & \dfrac{\cos\mu}{\cos\gamma} & 0 \\ 0 & -\sin\mu & 0 \end{bmatrix},\ H_1 = \begin{bmatrix} -g\sin\gamma \\ \dfrac{T}{mV\cos\gamma}\cos\alpha\sin\beta\cos\mu \\ \dfrac{T}{mV}\cos\alpha\sin\beta\sin\mu - \dfrac{g}{V}\cos\gamma \end{bmatrix},\ B_1 = \frac{1}{mV}\begin{bmatrix} V\cos\alpha\cos\beta & 0 & 0 \\ 0 & \dfrac{1}{\cos\gamma} & 0 \\ 0 & 0 & 1 \end{bmatrix}$$

are known (matrix and vector) functions, and

$$F_1 = \begin{bmatrix} L(X,U) \\ Y(X,U) \\ D(X,U) \end{bmatrix},\quad G_1 = \begin{bmatrix} T \\ \big(L(X,U) - T\sin\alpha\big)\sin\mu \\ \big(L(X,U) - T\sin\alpha\big)\cos\mu \end{bmatrix}$$

are functions containing the uncertain aerodynamic forces. Note that the intermediate control variables α and μ do not appear affine in the X_1 subsystem, which complicates the design somewhat. Because the control objective in this step is to track the smooth reference signal $X_1^{\mathrm{des}} = \begin{pmatrix} V^{\mathrm{des}} & \chi^{\mathrm{des}} & \gamma^{\mathrm{des}} \end{pmatrix}^T$ with $X_1 = \begin{pmatrix} V & \chi & \gamma \end{pmatrix}^T$, the tracking errors are defined as

$$Z_1 = \begin{bmatrix} z_{11} \\ z_{12} \\ z_{13} \end{bmatrix} = X_1 - X_1^{\text{des}} \tag{17}$$

To regulate Z_1 and z_{02} to zero, the following equation needs to be satisfied (Kanayama et al., 1990):

$$B_1 \hat{G}_1(X,U,X_2) = \begin{bmatrix} -c_{11} z_{11} \\ -V^{\text{ref}}\left(c_{02} z_{02} + c_{12} \sin z_{12}\right) \\ -c_{13} z_{13} \end{bmatrix} - A_1 \hat{F}_1 - H_1 + \dot{X}_1^{\text{des}} \tag{18}$$

where $\hat{F}_1$ is the estimate of F_1 and

$$\hat{G}_1(X,U,X_2) = \begin{bmatrix} T \\ \left(\hat{L}_0(X,U) + \hat{L}_\alpha(X,U)\alpha + T\sin\alpha\right)\sin\mu \\ \left(\hat{L}_0(X,U) + \hat{L}_\alpha(X,U)\alpha + T\sin\alpha\right)\cos\mu \end{bmatrix} \tag{19}$$

with the estimate of the lift force decomposed as $\hat{L}(X,U) = \hat{L}_0(X,U) + \hat{L}_\alpha(X,U)\alpha$

The estimate of the aerodynamic forces $\hat{F}_1$ is defined as

$$\hat{F}_1 = \Phi_{F_1}^T(X,U)\hat{\Theta}_{F_1} \tag{20}$$

where $\Phi_{F_1}^T$ is a known (chosen) regressor function and $\hat{\Theta}_{F_1}$ is a vector with unknown constant parameters. It is assumed that there exists a vector Θ_{F_1} such that

$$F_1 = \Phi_{F_1}^T(X,U)\Theta_{F_1} \tag{21}$$

This means the estimation error can be defined as $\tilde{\Theta}_{F_1} = \Theta_{F_1} - \hat{\Theta}_{F_1}$. We now need to determine the desired values α^{des} and μ^{des} . The right-hand side of Eq. (18) is entirely known, and so the left-hand side can be determined and the desired values can be extracted. This is done by introducing the coordinate transformation

$$x \equiv \left(\hat{L}_0(X,U) + \hat{L}_\alpha(X,U)\alpha + T\sin\alpha\right)\cos\mu \tag{22}$$

$$y \equiv \left(\hat{L}_0(X,U) + \hat{L}_\alpha(X,U)\alpha + T\sin\alpha\right)\sin\mu \tag{23}$$

which can be seen as a transformation from the two-dimensional polar coordinates

$$\hat{L}_0(X,U) + \hat{L}_\alpha(X,U)\alpha + T\sin\alpha$$

and μ to Cartesian coordinates x and y. The desired signals $\begin{bmatrix} T^{des,0} & y_0 & x_0 \end{bmatrix}^T$ are given by

$$B_1\begin{bmatrix} T^{\mathrm{des},0} \\ y_0 \\ x_0 \end{bmatrix} = \begin{bmatrix} -c_{11}z_{11} \\ -V^{\mathrm{ref}}\left(c_{02}z_{02} + c_{12}\sin z_{12}\right) \\ -c_{13}z_{13} \end{bmatrix} - A_1\hat{F}_1 - H_1 + \dot{X}_1^{\mathrm{des}} \tag{24}$$

Thus, the virtual control signals are equal to

$$\hat{L}_\alpha\left(X,U\right)\alpha^{\mathrm{des},0} = \sqrt{x_0^2 + y_0^2} - \hat{L}_0\left(X,U\right) - T\sin\alpha \tag{25}$$

and

$$\mu^{\mathrm{des},0} = \begin{cases} \arctan\left(y_0 / x_0\right) & \text{if } x_0 > 0 \\ \arctan\left(y_0 / x_0\right) + \pi & \text{if } x_0 < 0 \quad \text{and} \quad y_0 \geq 0 \\ \arctan\left(y_0 / x_0\right) - \pi & \text{if } x_0 < 0 \quad \text{and} \quad y_0 < 0 \\ \pi / 2 & \text{if } x_0 = 0 \quad \text{and} \quad y_0 > 0 \\ -\pi / 2 & \text{if } x_0 = 0 \quad \text{and} \quad y_0 < 0 \end{cases} \tag{26}$$

Filtering the virtual signals to account for magnitude, rate, and bandwidth limits will give the implementable virtual controls α^{des}, μ^{des} and their derivatives. The sideslip-angle command was already defined as $\beta^{\mathrm{ref}} = 0$, and thus $X_2^{\mathrm{des}} = \begin{bmatrix} \mu^{\mathrm{des}} & \alpha^{\mathrm{des}} & 0 \end{bmatrix}^T$ and its derivative are completely defined. However, care must be taken because the desired virtual control $\mu^{\mathrm{des},0}$ is undefined when both x_0 and y_0 are equal to zero, making the system momentarily uncontrollable. This sign change of $\hat{L}_0\left(X,U\right) + \hat{L}_\alpha\left(X,U\right)\alpha + T\sin\alpha$ can only occur at very low or negative angles of attack. This situation was not encountered during the maneuvers simulated in this study. To solve the problem altogether, the designer could measure the rate of change for x_0 and y_0 and devise a rule base set to change sign when these terms approach zero. Furthermore, problems will also occur at high angles of attack when the control effectiveness term $\hat{L}_\alpha$ will become smaller and eventually change sign. Possible solutions include limiting the angle-of-attack commands using the command filters or proper trajectory planning to avoid high-angle-of-attack maneuvers. Also note that so far in the control design process, we have not taken care of the update laws for the uncertain aerodynamic forces; they will be dealt with when the static control design is finalized.

3.3 Aerodynamic angle control

Now the reference signal $X_2^{\mathrm{des}} = [\mu^{\mathrm{des}} \quad \alpha^{\mathrm{des}} \quad \beta^{\mathrm{des}}]^T$ and its derivative have been found and we can move on to the next feedback loop. The available virtual controls in this step are the angular rates X_3. The relevant equations of motion for this part of the design are given by

$$\dot{X}_2 = A_2F_1\left(X,U\right) + B_2\left(X\right)X_3 + H_2\left(X\right) \tag{27}$$

where

$$A_2 = \frac{1}{mV}\begin{bmatrix} \tan\beta + \tan\gamma\sin\mu & \tan\gamma\cos\mu & 0 \\ \dfrac{-1}{\cos\beta} & 0 & 0 \\ 0 & 1 & 0 \end{bmatrix}, \quad B_2 = \begin{bmatrix} \dfrac{\cos\alpha}{\cos\beta} & 0 & \dfrac{\sin\alpha}{\cos\beta} \\ -\cos\alpha\tan\beta & 1 & -\sin\alpha\tan\beta \\ \sin\alpha & 0 & \cos\alpha \end{bmatrix}$$

$$H_2 = \frac{1}{mV}\begin{bmatrix} T\left(\sin\alpha\tan\gamma\sin\mu + \sin\alpha\tan\beta - \cos\alpha\sin\beta\tan\gamma\cos\mu\right) - \frac{g}{V}\tan\beta\cos\gamma\cos\mu \\ T\frac{\sin\alpha}{\cos\beta} + \frac{g}{V}\cos\gamma\cos\mu \\ -T\cos\alpha\cos\beta + \frac{g}{V}\cos\gamma\sin\mu \end{bmatrix}$$

are known (matrix and vector) functions. The tracking errors are defined as

$$Z_2 = X_2 - X_2^{\text{des}} \tag{28}$$

To stabilize the Z_2 subsystem, a virtual feedback control $X_3^{\text{des},0}$ is defined as

$$B_2 X_3^{\text{des},0} = -C_2 Z_2 - A_2\hat{F}_1 - H_2 + \dot{X}_2^{\text{des}}, \quad C_2 = C_2^T > 0 \tag{29}$$

The implementable virtual control (i.e., the reference signal for the inner loop) X_3^{des} and its derivative are again obtained by filtering the virtual control signal $X_3^{\text{des},0}$ with a second-order command-limiting filter.

3.4 Angular rate control

In the fourth step, an inner-loop feedback loop for the control of the body-axis angular rates $X_3 = \begin{bmatrix} p & q & r \end{bmatrix}^T$ is constructed. The control inputs for the inner loop are the control-surface deflections $U = \begin{bmatrix} \delta_e & \delta_a & \delta_r \end{bmatrix}^T$. The dynamics of the angular rates can be written as

$$\dot{X}_3 = A_3\left(F_3\left(X,U\right) + B_3\left(X\right)U\right) + H_3\left(X\right) \tag{30}$$

where

$$A_3 = \begin{bmatrix} c_3 & 0 & c_4 \\ 0 & c_7 & 0 \\ c_4 & 0 & c_9 \end{bmatrix}, \quad H_3 = \begin{bmatrix} \left(c_1 r + c_2 p\right)q \\ c_5 pr - c_6\left(p^2 - r^2\right) \\ \left(c_8 p - c_2 r\right)q \end{bmatrix}$$

are known (matrix and vector) functions, and

$$F_3 = \begin{bmatrix} \bar{L}_0 \\ \bar{M}_0 \\ \bar{N}_0 \end{bmatrix}, \quad B_3 = \begin{bmatrix} \bar{L}_{\delta_e} & \bar{L}_{\delta_a} & \bar{L}_{\delta_r} \\ \bar{M}_{\delta_e} & \bar{M}_{\delta_a} & \bar{M}_{\delta_r} \\ \bar{N}_{\delta_e} & \bar{N}_{\delta_a} & \bar{N}_{\delta_r} \end{bmatrix}$$

are unknown (matrix and vector) functions that have to be approximated. Note that for a more convenient presentation, the aerodynamic moments have been decomposed: for example,

$$\bar{M}\left(X,U\right) = \bar{M}_0\left(X,U\right) + \bar{M}_{\delta_e}\delta_e + \bar{M}_{\delta_a}\delta_a + \bar{M}_{\delta_r}\delta_r \tag{31}$$

where the higher-order control-surface dependencies are still contained in $\bar{M}_0(X,U)$. The control objective in this feedback loop is to track the reference signal $X_3^{\text{des}} = [p^{\text{ref}} \quad q^{\text{ref}} \quad r^{\text{ref}}]^T$ with the angular rates X_3. Defining the tracking errors

$$Z_3 = X_3 - X_3^{\text{des}} \tag{32}$$

and taking the derivatives results in

$$\dot{Z}_3 = A_3\left(F_3(X,U) + B_3(X)U\right) + H_3(X) - \dot{X}_3^{\text{des}} \tag{33}$$

To stabilize the system of Eq. (33), we define the desired control U^0 as

$$A_3\hat{B}_3U^0 = -C_3Z_3 - A_3\hat{F}_3 - H_3 + \dot{X}_3^{\text{des}}, \quad C_3 = C_3^T > 0 \tag{34}$$

where $\hat{F}_3$ and $\hat{B}_3$ are the estimates of the unknown nonlinear aerodynamic moment functions F_3 and B_3, respectively. The F-16 model is not over-actuated (i.e., the B_3 matrix is square). If this is not the case, some form of control allocation would be required (Enns, 1998, Durham, 1993). The estimates are defined as

$$\hat{F}_3 = \Phi_{F_3}^T(X,U)\hat{\Theta}_{F_3}, \quad \hat{B}_{3_i} = \Phi_{B_{3_i}}^T(X)\hat{\Theta}_{B_{3_i}}, \quad \text{for } i = 1,\cdots,3 \tag{35}$$

where $\Phi_{F_3}^T$ and $\Phi_{B_{3_i}}^T$ are the known regressor functions, $\hat{\Theta}_{F_3}$ and $\hat{\Theta}_{B_{3_i}}$ are vectors with unknown constant parameters, and $\hat{B}_{3_i}$ represents the ith column of $\hat{B}_3$. It is assumed that there exist vectors Θ_{F_3} and $\Theta_{B_{3_i}}$ such that

$$F_3 = \Phi_{F_3}^T(X,U)\Theta_{F_3}, \quad B_{3_i} = \Phi_{B_{3_i}}^T(X)\Theta_{B_{3_i}} \tag{36}$$

This means that the estimation errors can be defined as $\tilde{\Theta}_{F_3} = \Theta_{F_3} - \hat{\Theta}_{F_3}$ and $\tilde{\Theta}_{B_{3_i}} = \Theta_{B_{3_i}} - \hat{\Theta}_{B_{3_i}}$. The actual control U is found by applying a filter similar to Eq. (13) to U^0.

3.5 Update laws and stability properties

We have now finished the static part of our control design. In this section the stability properties of the control law are discussed and dynamic update laws for the unknown parameters are derived. Define the control Lyapunov function

$$\begin{aligned} V = {} & \frac{1}{2}\left(Z_0^TZ_0 + z_{11}^2 + \frac{2-2\cos z_{12}}{c_{02}} + z_{13}^2 + Z_2^TZ_2 + Z_3^TZ_3\right) + \\ & + \frac{1}{2}\left(\text{trace}\left(\tilde{\Theta}_{F_1}^T\Gamma_{F_1}^{-1}\tilde{\Theta}_{F_1}\right) + \text{trace}\left(\tilde{\Theta}_{F_3}^T\Gamma_{F_3}^{-1}\tilde{\Theta}_{F_3}\right)\right) + \sum_{i=1}^{3}\text{trace}\left(\tilde{\Theta}_{B_{3_i}}^T\Gamma_{B_{3_i}}^{-1}\tilde{\Theta}_{B_{3_i}}\right) \end{aligned} \tag{37}$$

with the update gains matrices $\Gamma_{F_1} = \Gamma_{F_1}^T > 0$, $\Gamma_{F_3} = \Gamma_{F_3}^T > 0$, and $\Gamma_{B_{3_i}} = \Gamma_{B_{3_i}}^T > 0$. Taking the derivative of V along the trajectories of the closed-loop system gives

$$\begin{aligned}\dot{V} = &-c_{01}z_{01}^2 + z_{02}z_{01}\dot{\chi} + \left(V - V^{\text{des},0}\right)z_{01} + z_{02}\left(-z_{01}\dot{\chi} + V^{\text{ref}}\sin z_{12}\right) - c_{03}z_{03}^2 - V\left(\sin\gamma - \sin\gamma^{\text{des},0}\right)z_{03} + \\ &- c_{11}z_{11}^2 - V^{\text{ref}}\left(\sin z_{12}z_{02} + \frac{c_{12}}{c_{02}}\sin^2 z_{12}\right) - c_{13}z_{13}^2 + Z_1^T\left(A_1\Phi_{F_1}^T\tilde{\Theta}_{F_1} + B_1\left(G_1\left(X_2\right) - \hat{G}_1\left(X_2\right)\right)\right) + \\ &+ Z_1^T B_1\left(\hat{G}_1\left(X_2\right) - \hat{G}_1\left(X_2^{\text{des},0}\right)\right) - Z_2^T C_2 Z_2 + Z_2^T A_2\Phi_{F_1}^T\tilde{\Theta}_{F_1} + Z_2^T B_2\left(X_3 - X_3^{\text{des},0}\right) - Z_3^T C_3 Z_3 + \\ &+ Z_3^T A_3\left(\Phi_{F_3}^T\tilde{\Theta}_{F_3} + \sum_{i=1}^{3}\Phi_{B_{3_i}}^T\tilde{\Theta}_{B_{3_i}}U_i\right) + Z_3^T A_3\hat{B}_3\left(U - U^0\right) - \text{trace}\left(\dot{\hat{\Theta}}_{F_1}^T\Gamma_{F_1}^{-1}\tilde{\Theta}_{F_1}\right) - \text{trace}\left(\dot{\hat{\Theta}}_{F_3}^T\Gamma_{F_3}^{-1}\tilde{\Theta}_{F_3}\right) + \\ &- \sum_{i=1}^{3}\text{trace}\left(\dot{\hat{\Theta}}_{B_{3_i}}^T\Gamma_{B_{3_i}}^{-1}\tilde{\Theta}_{B_{3_i}}\right)\end{aligned} \tag{38}$$

To cancel the terms in Eq. (38), depending on the estimation errors, we select the update laws

$$\dot{\hat{\Theta}}_{F_1} = \Gamma_{F_1}\Phi_{F_1}\left(A_{1a}^T Z_1 + A_2^T Z_2\right), \quad \dot{\hat{\Theta}}_{F_3} = \Gamma_{F_3}\Phi_{F_3}A_3^T Z_3, \quad \dot{\hat{\Theta}}_{B_{3_i}} = \text{proj}_{B_{3_i}}\left(\Gamma_{B_{3_i}}\Phi_{B_{3_i}}A_3^T Z_3 U_i\right) \tag{39}$$

with $A_{1a}\Phi_{F_1}^T\tilde{\Theta}_{F_1} = A_1\Phi_{F_1}^T\tilde{\Theta}_{F_1} + B_1\left(G_1\left(X_2\right) - \hat{G}_1\left(X_2\right)\right)$

The update laws for $\hat{B}_3$ include a projection operator (Ioannou and Sun, 1995) to ensure that certain elements of the matrix do not change sign and full rank is maintained always. For most elements, the sign is known based on physical principles. Substituting the update laws in Eq. (38) leads to

$$\begin{aligned}\dot{V} = &-c_{01}z_{01}^2 - c_{03}z_{03}^2 - c_{11}z_{11}^2 - -V^{\text{ref}}\frac{c_{12}}{c_{02}}\sin^2 z_{12} - c_{13}z_{13}^2 - Z_2^T C_2 Z_2 - Z_3^T C_3 Z_3 + \left(V - V^{\text{des},0}\right)z_{01} + \\ &- V\left(\sin\gamma - \sin\gamma^{\text{des},0}\right)z_{03} + Z_1^T B_1\left(G_1\left(X_2\right) - \hat{G}_1\left(X_2^{\text{des},0}\right)\right) + Z_2^T B_2\left(X_3 - X_3^{\text{des},0}\right) + Z_3^T A_3\hat{B}_3\left(U - U^0\right)\end{aligned} \tag{40}$$

where the first line is already negative semi-definite, which we need to prove stability in the sense of Lyapunov. Because our Lyapunov function V equation (37) is not radially unbounded, we can only guarantee local asymptotic stability (Kanayama et al., 1990). This is sufficient for our operating area if we properly initialize the control law to ensure $z_{12} \le \pm\pi/2$. However, we also have indefinite error terms due to the tracking errors and due to the command filters used in the design. As mentioned before, when no rate or magnitude limits are in effect, the difference between the input and output of the filters can be made small by selecting the bandwidth of the filters to be sufficiently larger than the bandwidth of the input signal. Also, when no limits are in effect and the small bounded difference between the input and output of the command filters is neglected, the feedback controller designed in the previous sections will converge the tracking errors to zero (for proof, see (Farrell et al., 2005, Sonneveldt et al., 2007, Yip, 1997)).

Naturally, when control or state limits are in effect, the system will in general not track the reference signal asymptotically. A problem with adaptive control is that this can lead to corruption of the parameter-estimation process, because the tracking errors that are driving this process are no longer caused by the function approximation errors alone (Farrell et al., 2003). To solve this problem we will use a modified definition of the tracking errors in the update laws in which the effect of the magnitude and rate limits has been removed, as suggested in (Farrell et al., 2005, Sonneveldt et al., 2006). Define the modified tracking errors

$$\tilde{Z}_1 = Z_1 - \Xi_1, \quad \tilde{Z}_2 = Z_2 - \Xi_2, \quad \tilde{Z}_3 = Z_3 - \Xi_3 \tag{41}$$

with the linear filters

$$\begin{aligned}
\dot{\Xi}_1 &= -C_1\Xi_1 + B_1\left(\hat{G}_1\left(X,U,X_2\right) - \hat{G}_1\left(X,U,X_2^{\text{des},0}\right)\right) \\
\dot{\Xi}_2 &= -C_2\Xi_2 + B_2\left(X_3 - X_3^{\text{des},0}\right) \\
\dot{\Xi}_3 &= -C_3\Xi_3 + A_3\hat{B}_3\left(U - U^0\right)
\end{aligned} \tag{42}$$

The modified errors will still converge to zero when the constraints are in effect, which means the robustified update laws look like

$$\dot{\hat{\Theta}}_{F_1} = \Gamma_{F_1}\Phi_{F_1}\left(A_{1a}^T Z_1 + A_2^T Z_2\right), \quad \dot{\hat{\Theta}}_{F_3} = \Gamma_{F_3}\Phi_{F_3}A_3^T Z_3, \quad \dot{\hat{\Theta}}_{B_{3_i}} = \text{proj}_{B_{3_i}}\left(\Gamma_{B_{3_i}}\Phi_{B_{3_i}}A_3^T Z_3 U_i\right) \tag{43}$$

To better illustrate the structure of the control system, a scheme of the adaptive inner-loop controller is shown in Fig. 2.

4. Model identification

To simplify the approximation of the unknown aerodynamic force and moment functions, thereby reducing computational load, the flight envelope is partitioned into multiple connecting operating regions called hyperboxes or clusters. This can be done manually using a priori knowledge of the nonlinearity of the system, automatically using nonlinear optimization algorithms that cluster the data into hyperplanar or hyperellipsoidal clusters (Babuška, 1998) or a combination of both. In each hyperbox a locally valid linear-in-the-parameters nonlinear model is defined, which can be estimated using the update laws of the Lyapunov-based control laws. The aerodynamic model can be partitioned using different state variables, the choice of which depends on the expected nonlinearities of the system. In this study we use B-spline neural networks (Cheng et al., 1999, Ward et al., 2003) (i.e., radial basis function neural networks with B-spline basis functions) to interpolate between the local nonlinear models, ensuring smooth transitions. In the previous section we defined parameter update laws equation (43) for the unknown aerodynamic functions, which were written as

$$\hat{F}_1 = \Phi_{F_1}^T\left(X,U\right)\hat{\Theta}_{F_1}, \quad \hat{F}_3 = \Phi_{F_3}^T\left(X,U\right)\hat{\Theta}_{F_3}, \quad \hat{B}_{3_i} = \Phi_{B_{3_i}}^T\left(X\right)\hat{\Theta}_{B_{3_i}} \tag{44}$$

Now we will further define these unknown vectors and known regressor vectors. The total force approximations are defined as

$$\begin{aligned}
\hat{L} &= \bar{q}S\left(\hat{C}_{L_0}\left(\alpha,\beta\right) + \hat{C}_{L_\alpha}\left(\beta,\delta_e\right)\alpha + \hat{C}_{L_q}\left(\alpha\right)\frac{q\bar{c}}{2V} + \hat{C}_{L_{\delta_e}}\left(\alpha,\beta\right)\delta_e\right) \\
\hat{Y} &= \bar{q}S\left(\hat{C}_{Y_0}\left(\alpha,\beta,\delta_e\right) + \hat{C}_{Y_p}\left(\alpha,\beta\right)\frac{pb}{2V} + \hat{C}_{Y_r}\left(\alpha,\beta\right)\frac{rb}{2V} + \hat{C}_{Y_{\delta_a}}\left(\alpha,\beta\right)\delta_a + \hat{C}_{Y_{\delta_r}}\left(\alpha,\beta\right)\delta_r\right) \\
\hat{D} &= \bar{q}S\left(\hat{C}_{D_0}\left(\alpha,\beta,\delta_e\right) + \hat{C}_{D_{\delta_e}}\left(\alpha,\beta\right)\delta_e\right)
\end{aligned} \tag{45}$$

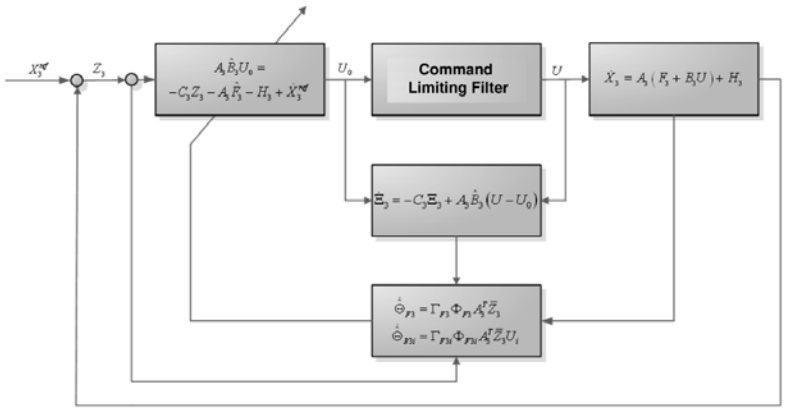

Fig. 2. Inner-loop control system

and the moment approximations are defined as

$$\begin{aligned}
\hat{\bar{L}} &= \bar{q}S\left(\hat{C}_{\bar{L}_0}(\alpha,\beta,\delta_e)+\hat{C}_{\bar{L}_p}(\alpha,\beta)\frac{pb}{2V}+\hat{C}_{\bar{L}_r}(\alpha,\beta)\frac{rb}{2V}+\hat{C}_{\bar{L}_{\delta_e}}(\alpha,\beta)\delta_e+\hat{C}_{\bar{L}_{\delta_a}}(\alpha,\beta)\delta_a+\hat{C}_{\bar{L}_{\delta_r}}(\alpha,\beta)\delta_r\right)\\
\hat{\bar{M}} &= \bar{q}S\left(\hat{C}_{\bar{M}_0}(\alpha,\beta)+\hat{C}_{\bar{M}_q}(\alpha)\frac{q\bar{c}}{2V}+\hat{C}_{\bar{M}_{\delta_e}}(\alpha,\beta)\delta_e\right)\\
\hat{\bar{N}} &= \bar{q}S\left(\hat{C}_{\bar{N}_0}(\alpha,\beta,\delta_e)+\hat{C}_{\bar{N}_p}(\alpha,\beta)\frac{pb}{2V}+\hat{C}_{\bar{N}_r}(\alpha,\beta)\frac{rb}{2V}+\hat{C}_{\bar{N}_{\delta_e}}(\alpha,\beta)\delta_e+\hat{C}_{\bar{N}_{\delta_a}}(\alpha,\beta)\delta_a+\hat{C}_{\bar{N}_{\delta_r}}(\alpha,\beta)\delta_r\right)
\end{aligned} \tag{46}$$

Note that these approximations do not account for asymmetric failures that will introduce coupling of the longitudinal and lateral motions of the aircraft. If a failure occurs that introduces a parameter dependency that is not included in the approximation, stability can no longer be guaranteed. It is possible to include extra cross-coupling terms, but this is beyond the scope of this paper. The total nonlinear function approximations are divided into simpler linear-in-the parameter nonlinear coefficient approximations: for example,

$$\hat{C}_{L_0}(\alpha,\beta)=\varphi_{C_{L_0}}^T(\alpha,\beta)\hat{\theta}_{C_{L_0}} \tag{47}$$

where the unknown parameter vector $\hat{\theta}_{C_{L_0}}$ contains the network weights (i.e., the unknown parameters), and $\varphi_{C_{L_0}}$ is a regressor vector containing the B-spline basis functions (Sonneveldt et al., 2007). All other coefficient estimates are defined in similar fashion. In this case a two-dimensional network is used with input nodes for α and β. Different scheduling parameters can be selected for each unknown coefficient. In this study we used third-order B-splines spaced 2.5 deg and one or more of the selected scheduling variables α, β and δ_e. Following the notation of Eq. (47), we can write the estimates of the aerodynamic forces and moments as

$$\begin{aligned}
&\hat{L}=\Phi_L^T(\alpha,\beta,\delta_e)\hat{\Theta}_L,\quad \hat{Y}=\Phi_Y^T(\alpha,\beta,\delta_e)\hat{\Theta}_Y,\quad \hat{D}=\Phi_D^T(\alpha,\beta,\delta_e)\hat{\Theta}_D\\
&\hat{\bar{L}}=\Phi_{\bar{L}}^T(\alpha,\beta,\delta_e)\hat{\Theta}_{\bar{L}},\quad \hat{\bar{M}}=\Phi_{\bar{M}}^T(\alpha,\beta,\delta_e)\hat{\Theta}_{\bar{M}},\quad \hat{\bar{N}}=\Phi_{\bar{N}}^T(\alpha,\beta,\delta_e)\hat{\Theta}_{\bar{N}}
\end{aligned} \tag{48}$$

which is a notation equivalent to the one used in Eq. (44). Therefore, the update laws equation (43) can indeed be used to adapt the B-spline network weights. In practice nonparametric uncertainties such as 1) un-modeled structural vibrations 2) measurement noise, 3) computational round-off errors and sampling delays, and 4) time variations of the unknown parameters, can result in parameter drift. One approach to avoiding parameter drift taken here is to stop the adaptation process when the training error is very small (i.e. a dead zones (Babuška, 1998, Karason and Annaswamy, 1994)).

5. Simulation results

This section presents the simulation results from the application of the flight-path controller developed in the previous sections to the high-fidelity, six-degree-of-freedom F-16 model of Sec. 2. Both the control law and the aircraft model are written as *C* S-functions in MATLAB/Simulink. The simulations are performed at three different starting flight conditions with the trim conditions: 1) h= 5000 m, V= 200 m/s, and a=θ=2.774 deg; 2) h=0 m, V =250 m/s, and a=θ=2.406 deg; and 3) h= 2500 m, V= 150 m/s, and a=θ=0.447 deg; where h is the altitude of the aircraft, and all other trim states are equal to zero.
Furthermore, two maneuvers are considered: 1) a climbing helical path and 2) a reconnaissance and surveillance maneuver. The latter maneuver involves turns in both directions and some altitude changes. The simulations of both maneuvers last 300 s. The reference trajectories are generated with second-order linear filters to ensure smooth trajectories. To evaluate the effectiveness of the online model identification, all maneuvers will also be performed with a ±30% deviation in all aerodynamic stability and control derivatives used by the controller (i.e., it is assumed that the onboard model is very inaccurate). Finally, the same maneuvers are also simulated with a lockup at ±10 deg of the left aileron.

5.1 Control parameter tuning

We start with the selection of the gains of the static control law and the bandwidths of the command filters. Lyapunov stability theory only requires the control gains to be larger than zero, but it is natural to select the largest gains of the inner loop. Larger gains will, of course, result in smaller tracking errors, but at the cost of more control effort. It is possible to derive certain performance bounds that can serve as guidelines for tuning (see, for example, Krstić, et al., 1993, Sonneveldt et al., 2007). However, getting the desired closed-loop response is still an extensive trial-and-error procedure. The control gains were selected as $c_{01} = 0.1$, $c_{02} = 10^{-5}$, $c_{03} = 0.5$, $c_{11} = 0.01$, $c_{12} = 2.5$, $c_{13} = 0.5$, $C_2 = \mathrm{diag}(1,1,1)$, $C_3 = \mathrm{diag}(2,2,2)$.

The bandwidths of the command filters for the actual control variables δ_e, δ_a, and δ_r are chosen to be equal to the bandwidths of the actuators, which are given in (Sonneveldt et al., 2007). The outer-loop filters have the smallest bandwidths. The selection of the other bandwidths is again trial and error. A higher bandwidth in a certain feedback loop will result in more aggressive commands to the next feedback loop. All damping ratios are equal to 1.0. It is possible to add magnitude and rate limits to each of the filters. In this study magnitude limits on the aerodynamic roll angle μ and the flight-path angle γ are used to avoid singularities in the control laws. Rate and magnitude limits equal to those of the actuators are enforced on the actual control variables.

The selected command-filter parameters can be found back in Table 1. As soon as the controller gains and command-filter parameters have been defined, the update law gains can be selected. Again, the theory only requires that the gains should be larger than zero. Larger update gains means higher learning rates and thus more rapid changes in the B-spline network weights.

5.2 Manoeuvre 1: upward spiral

In this section the results of the numerical simulations of the first test maneuver, the climbing helical path, are discussed. For each of the three flight conditions, five cases are considered: nominal, the aerodynamic stability and control derivatives used in the control law perturbed with +30% and with -30% with respect to the real values of the model, a lockup of the left aileron at +10 deg, and a lockup at -10 deg. No actuator sensor information is used. In Fig. 3 the results are plotted of the simulation without uncertainty, starting at flight condition 1. The maneuver involves a climbing spiral to the left with an increase in airspeed. It can be seen that the control law manages to track the reference signal very well and closed-loop tracking is achieved. The sideslip angle does not become any larger than ±0.02 deg. The aerodynamic roll angle does reach the limit set by the command filter, but this has no consequences for the performance. The use of dead zones ensures that the parameter update laws are indeed not updating during this maneuver without any uncertainties. The responses at the two other flight conditions are virtually the same, although less thrust is needed due to the lower altitude of flight condition 2 and the lower airspeed of flight condition 3. The other control surfaces are also more efficient. This is illustrated in Tables 2–4, in which the mean absolute values (MAVs) of the outer-loop tracking errors, control-surface deflections, and thrust can be found. Plots of the parameter-estimation errors are not included. However, the errors converge to constant values, but not to zero, as is common with Lyapunov-based update laws (Sonneveldt et al., 2007, Page and Steinberg, 1999).

Command variable	ω_n, rad/s	Magnitude limit	Rate limit
V^{des}	5	——	——
γ^{des}	3	±80 deg	——
μ^{des}	8	±80 deg	——
α^{des}	8	——	——
p^{des}	20	——	——
q^{des}	20	——	——
r^{des}	10	——	——
δ_e	40.4	±25 deg	±60 deg/s
δ_a	40.4	±21.5 deg	±80 deg/s
δ_r	40.4	±30 deg	±120 deg/s
T	10	[1000–100,000] N	±40,000 N/s

Table 1. Command-filter parameters

Case	$(z_{01}, z_{02}, z_{03})^{MAV}$, m	$(\delta_e, \delta_a, \delta_r)^{MAV}$, deg	T^{MAV}, N
Nominal	(0.33,0.24,0.24)	(4.63, 0.12, 0.10)	$5.59e+04$
+30% uncertainty	(4.56,3.75,1.07)	(4.59, 0.13, 0.11)	$5.57e+04$
−30% uncertainty	(5.15,3.88,1.10)	(4.68, 0.16, 0.11)	$5.62e+04$
+10% deg, locked left aileron	(0.39,0.32,0.78)	(4.63, 0.56, 0.74)	$5.59e+04$
−10% deg, locked left aileron	(0.31,0.25,1.12)	(4.63, 0.46, 1.16)	$5.59e+04$

Table 2. Manoeuvre 1 at flight condition 1: mean absolute value of tracking errors and control inputs

Case	$(z_{01}, z_{02}, z_{03})^{MAV}$, m	$(\delta_e, \delta_a, \delta_r)^{MAV}$, deg	T^{MAV}, N
Nominal	(0.30,0.23,0.21)	(3.97, 0.14, 0.21)	$3.14e+04$
+30% uncertainty	(1.55,1.33,0.41)	(3.96, 0.15, 0.23)	$3.14e+04$
−30% uncertainty	(2.01,1.53,0.52)	(3.98, 0.15, 0.20)	$3.14e+04$
+10% deg, locked left aileron	(0.36,0.33,0.72)	(3.97, 0.25, 1.20)	$3.14e+04$
−10% deg, locked left aileron	(0.30,0.28,1.01)	(3.96, 0.40, 1.52)	$3.14e+04$

Table 3. Manoeuvre 1 at flight condition 2: mean absolute value of tracking errors and control inputs

Case	$(z_{01}, z_{02}, z_{03})^{MAV}$, m	$(\delta_e, \delta_a, \delta_r)^{MAV}$, deg	T^{MAV}, N
Nominal	(0.33,0.22,0.27)	(3.37, 0.08, 0.08)	$4.41e+04$
+30% uncertainty	(2.01,1.43,0.61)	(3.40, 0.10, 0.08)	$4.44e+04$
−30% uncertainty	(2.16,1.49,0.77)	(3.38, 0.09, 0.08)	$4.41e+04$
+10% deg, locked left aileron	(0.32,0.33,0.29)	(3.38, 0.08, 0.09)	$4.41e+04$
−10% deg, locked left aileron	(0.34,0.24,0.30)	(3.38, 0.08, 0.09)	$4.41e+04$

Table 4. Manoeuvre 1 at flight condition 3: mean absolute value of tracking errors and control inputs

The response of the closed-loop system during the same maneuver starting at flight condition 1, but with +30% uncertainties in the aerodynamic coefficients, is shown in Fig. 4. It can be observed that the tracking errors of the outer loop are now much larger, but in the end, the steady-state tracking error converges to zero. The sideslip angle still remains within 0.02 deg. Some small oscillations are visible in Fig. 4j, but these stay well within the rate and magnitude limits of the actuators. In Tables 2–4 the MAVs of the tracking errors and control inputs are shown for all flight conditions. As was already seen in the plots, the average tracking errors increase, but the magnitude of the control inputs stays approximately the same. The same simulations have been performed for a -30% perturbation in the stability and control derivatives used by the control law, and the results are also shown in the tables. It appears that underestimated initial values of the unknown parameters lead to larger tracking errors than overestimates for this maneuver. Finally, the maneuver is performed with the left aileron locked at ±10 deg [i.e., $\delta_a^{\text{damaged}} = 0.5\left(\delta_a \pm 10\pi / 180\right)$]. Figure 5 shows the response at flight condition 3 with the aileron locked at -10 deg.

Except for some small oscillations in the response of roll rate p, there is no real change in performance visible; this is confirmed by the numbers of Table 4. However, from Tables 2 and 3 we observe that aileron and rudder deflections become larger with both locked aileron failure cases, whereas tracking performance hardly declines.

5.3 Manoeuvre 2: reconnaissance

The second maneuver, called reconnaissance and surveillance, involves turns in both directions and altitude changes, but airspeed is kept constant. Plots of the simulation at flight condition 3 with -30% uncertainties are shown in Fig. 6. Tracking performance is again excellent and the steady-state tracking errors converge to zero. There are some small oscillations in the rudder deflection, but these are within the limits of the actuator. We compare the MAVs of the tracking errors and control inputs with those for the nominal case in Table 5 and observe that the average tracking errors have not increased much for this case. The degradation of performance for the uncertainty cases is somewhat worse at the other two flight conditions, as can be seen in Tables 6 and 7. The sideslip angle always remains within 0.05 deg for all flight conditions and uncertainties. Corresponding with the

results of maneuver 1, overestimation of the unknown parameters again leads to smaller tracking errors. Simulations of maneuver 2 with the locked aileron are also performed. Figure 7 shows the results for flight condition 1 with a locked aileron at _10 deg. Some very small oscillations are again visible in the roll rate, aileron, and rudder responses, but tracking performance is good and steady-state convergence is achieved.
Table 6 confirms that the results of the simulations with actuator failure hardly differ from the nominal case. There is only a small increase in the use of the lateral control surfaces. The same holds at the other flight conditions, as can be seen in Tables 5 and 7.

Case	$(z_{01}, z_{02}, z_{03})^{MAV}$, m	$(\delta_e, \delta_a, \delta_r)^{MAV}$, deg	T^{MAV}, N
Nominal	(0.49,0.40,0.56)	(2.39, 0.12, 0.12)	$2.33e+04$
+30% uncertainty	(0.97,0.78,0.54)	(2.39, 0.12, 0.13)	$2.33e+04$
−30% uncertainty	(0.97,0.56,0.85)	(2.40, 0.13, 0.12)	$2.33e+04$
+10% deg, locked left aileron	(0.48,0.40,0.58)	(2.39, 0.12, 0.13)	$2.33e+04$
−10% deg, locked left aileron	(0.49,0.40,0.56)	(2.40, 0.13, 0.13)	$2.33e+04$

Table 5. Manoeuvre 2 at flight condition 3: mean absolute value of tracking errors and control inputs

Case	$(z_{01}, z_{02}, z_{03})^{MAV}$, m	$(\delta_e, \delta_a, \delta_r)^{MAV}$, deg	T^{MAV}, N
Nominal	(0.42,0.39,0.46)	(3.17, 0.16, 0.13)	$2.25e+04$
+30% uncertainty	(2.69,2.30,1.13)	(3.16, 0.16, 0.14)	$2.25e+04$
−30% uncertainty	(3.02,2.40,1.12)	(3.19, 0.18, 0.14)	$2.25e+04$
+10% deg, locked left aileron	(0.43,0.40,0.45)	(3.17, 0.17, 0.16)	$2.25e+04$
−10% deg, locked left aileron	(0.42,0.39,0.46)	(3.17, 0.17, 0.15)	$2.25e+04$

Table 6. Manoeuvre 2 at flight condition 1: mean absolute value of tracking errors and control inputs

Case	$(z_{01}, z_{02}, z_{03})^{MAV}$, m	$(\delta_e, \delta_a, \delta_r)^{MAV}$, deg	T^{MAV}, N
Nominal	(0.58,0.49,0.34)	(2.95, 0.18, 0.21)	$1.62e+04$
+30% uncertainty	(1.27,1.10,0.48)	(2.95, 0.19, 0.22)	$1.62e+04$
−30% uncertainty	(1.73,1.24,0.55)	(2.97, 0.19, 0.21)	$1.61e+04$
+10% deg, locked left aileron	(0.58,0.50,0.35)	(2.95, 0.20, 0.22)	$1.62e+04$
−10% deg, locked left aileron	(0.59,0.51,0.34)	(2.95, 0.22, 0.22)	$1.62e+04$

Table 7. Manoeuvre 2 at flight condition 2: mean absolute value of tracking errors and control inputs

6. Conclusions

In this paper a nonlinear adaptive flight-path control system is designed for a high-fidelity F-16 model. The controller is based on a backstepping approach with four feedback loops that are designed using a single control Lyapunov function to guarantee stability. The uncertain aerodynamic forces and moments of the aircraft are approximated online with B-spline neural networks for which the weights are adapted by Lyapunov-based update laws. Numerical simulations of two test maneuvers were performed at several flight conditions to verify the performance of the control law. Actuator failures and uncertainties in the stability and control derivatives are introduced to evaluate the parameter-estimation process. The results show that trajectory control can still be accomplished with these uncertainties and failures, and good tracking performance is maintained. Compared with other Lyapunov-

based trajectory control designs, the present approach is much simpler to apply and the online estimation process is more robust to saturation effects. Future studies will focus on the actual trajectory generation and the extension to formation-flying control.

Appendix constraint adaptive backstepping

Backstepping [21] is a systematic, Lyapunov-based method for nonlinear control design, which can be applied to nonlinear systems that can be transformed into lower-triangular form, such as the system of Eq. (A.1):

$$\dot{x}_1 = f(x_1) + g(x_1)x_2 \tag{A.1}$$

The name "backstepping" refers to the recursive nature of the control law design procedure. Using the backstepping procedure, a control law is recursively constructed, along with a control Lyapunov function (CLF) to guarantee global stability. For the system Eq. (A.1), the aim of the design procedure is to bring the state vector x_1 to the origin. The first step is to consider x_2 as the *virtual* control of the scalar x_1 subsystem and to find a desired virtual control law $\alpha_1(x_1)$ that stabilizes this subsystem by using the control Lyapunov function $V_1(x_1)$:

$$V_1(x_1) = \frac{1}{2}x_1^2 \tag{A.2}$$

The time derivative of this CLF is negative definite

$$\dot{V}_1(x_1) = \frac{\partial V_1(x_1)}{\partial x_1}\left[f(x_1) + g(x_1)\alpha_1(x_1)\right] < 0, \qquad x_1 \neq 0 \tag{A.3}$$

If only the virtual control law

$$x_2 = \alpha_1(x_1) \tag{A.4}$$

could be satisfied. The key property of backstepping is that we can now "step back" through the system. If the error between x_2 and its desired value is defined as

$$z = x_2 - \alpha_1(x_1) \tag{A.5}$$

the system Eq. (6) can be rewritten in terms of this error state

$$\begin{aligned} \dot{x}_1 &= f(x_1) + g(x_1)\left[\alpha_1(x_1) + z\right] \\ \dot{z} &= u - \frac{\partial \alpha_1(x_1)}{\partial x_1}\left(f(x_1) + g(x_1)\left[\alpha_1(x_1) + z\right]\right) \end{aligned} \tag{A.6}$$

The control Lyapunov function Eq. (A.2) can now be expanded with a term penalizing the error state z

$$V_2(x_1, z) = V_1(x_1) + \frac{1}{2}z^2 \tag{A.7}$$

In simplified notation the time derivative of V_2 is equal to

$$\begin{aligned}\dot{V}_2 &= \frac{\partial V_1}{\partial x_1}\left[f + g(\alpha_1 + z)\right] + z\left(u - \frac{\partial \alpha_1}{\partial x_1}\left[f + g(\alpha_1 + z)\right]\right) \\ &= \frac{\partial V_1}{\partial x_1}\left[f + g\alpha_1\right] + z\left(\frac{\partial V_1}{\partial x_1}g + u - \frac{\partial \alpha_1}{\partial x_1}\left[f + g(\alpha_1 + z)\right]\right)\end{aligned} \tag{A.8}$$

which can be rendered negative definite with the control law

$$u = -cz + \frac{\partial \alpha_1}{\partial x_1}\left[f + g(\alpha_1 + z)\right] - \frac{\partial V_1}{\partial x_1}g, \quad c > 0 \tag{A.9}$$

This design procedure can also be used for a system with a chain of integrators. The only difference is that there will be more virtual states to "backstep" through. Starting with the state "farthest" from the actual control, each step of the backstepping technique can be broken up into three parts: 1. Introduce a virtual control α_1 and an error state z, and rewrite the current state equation in terms of these; 2. choose a CLF for the system, treating it as a final stage; 3) choose an equation for the virtual control that makes the CLF stabilizable.
The CLF is augmented at subsequent steps to reflect the presence of new virtual states, but the same three stages are followed at each step. Hence, backstepping is a recursive design procedure.
For systems with parametric uncertainties there exists a method called adaptive backstepping (Kannelakopoulos et al., 1991), which achieves boundedness of the closed-loop states and convergence of the tracking error to zero.
Consider the parametric strict-feedback system

$$\begin{aligned}\dot{x}_1 &= x_2 + \varphi_1^T(x_1)\theta \\ &\vdots \\ \dot{x}_{n-1} &= x_n + \varphi_{n-1}^T(x_1, \cdots, x_{n-1})\theta \\ \dot{x}_n &= \beta(x)u + \varphi_n^T(x)\theta\end{aligned} \tag{A.10}$$

where $\beta(x) \neq 0$ for all $x \in \mathbb{R}^n$, θ is a vector of unknown constant parameters, and φ_i are known (smooth) function vectors. The control objective is to asymptotically track a given reference $y_r(t)$ with x_1. All derivatives of $y_r(t)$ are assumed to be known.
The adaptive backstepping design procedure is similar to the normal backstepping procedure, only this time a control law (static part) and a *parameter update law* (dynamic part) are designed along with a control Lyapunov function to guarantee global stability. The control law makes use of a parameter estimate $\hat{\theta}$, which is constantly adapted by the dynamic parameter update law. Furthermore, the control Lyapunov function now contains an extra term that penalizes the parameter estimation error $\tilde{\theta} = \theta - \hat{\theta}$.
Theorem A.1 (Adaptive Backstepping Method): To stabilize the system Eq. (A.9) an error variable is introduced for each state

$$z_i = x_i - y_r^{(i-1)} - \alpha_{i-1} \tag{A.11}$$

along with a virtual control law

$$\alpha_i\left(\bar{x}_i,\hat{\theta},\bar{y}_r^{(i-1)}\right)=-c_i z_i-z_{i-1}-\omega_i^T\hat{\theta}+\sum_{k=1}^{i-1}\left(\frac{\partial\alpha_{i-1}}{\partial x_k}x_{k+1}+\frac{\partial\alpha_{i-1}}{\partial y_r^{(k-1)}}y_r^{(k)}\right)+\frac{\partial\alpha_{i-1}}{\partial\hat{\theta}}\Gamma\tau_i+\sum_{k=2}^{i-1}\frac{\partial\alpha_{i-1}}{\partial\hat{\theta}}\Gamma\omega_i z_k \quad \text{(A.12)}$$

for $i=1,2,\cdots,n$, where the tuning function τ_i and the regressor vectors ω_i are defined as

$$\tau_i\left(\bar{x}_i,\hat{\theta},y_r^{(i-1)}\right)=\tau_{i-1}+\omega_i z_i \quad \text{(A.13)}$$

and

$$\omega_i\left(\bar{x}_i,\hat{\theta},y_r^{(i-2)}\right)=\varphi_i-\sum_{k=1}^{i-1}\frac{\partial\alpha_{i-1}}{\partial x_k}\varphi_k \quad \text{(A.14)}$$

where $\bar{x}_i=\left(x_1,x_2,\cdots,x_i\right)$, $\bar{y}_r^{(i)}=\left(y_r,\dot{y}_r,\cdots,y_r^{(i)}\right)$. $c_i>0$ are design constants. With these new variables the control and adaptation laws can be defined as

$$u=\frac{1}{\beta(x)}\left[\alpha_n\left(x,\hat{\theta},\bar{y}_r^{(n-1)}\right)+y_r^{(n)}\right] \quad \text{(A.15)}$$

and

$$\dot{\hat{\theta}}=\Gamma\tau_n\left(x,\hat{\theta},\bar{y}_r^{(n-1)}\right)=\Gamma W z \quad \text{(A.16)}$$

where $\Gamma=\Gamma^T>0$ is the adaptation gain matrix and W the regressor matrix

$$W\left(z,\hat{\theta}\right)=\left(\omega_1,\cdots,\omega_i\right) \quad \text{(A.17)}$$

The control law Eq. (A.15) together with the update law Eq. (A.17) renders the derivative of the Lyapunov function

$$V=\frac{1}{2}\sum_{i=1}^{n}z_i^2+\frac{1}{2}\tilde{\theta}^T\Gamma^{-1}\tilde{\theta} \quad \text{(A.18)}$$

negative definite and thus this adaptive controller guarantees global boundedness of $x(t)$ and asymptotically tracking of a given reference $y_r(t)$ with x_1.
Proof of this theorem can be found in Sec. 4.3 of (Krstić et al., 1992).
The standard adaptive backstepping procedure as has been discussed so far has a number of drawbacks.

1. The analytic calculation of the virtual control derivatives is tedious, especially for large systems;
2. The procedure can only handle systems that can be transformed into a lower-triangular form;
3. Constraints on the inputs and states are not taken into account.

The third drawback can be a major problem when designing for flight control, because the actuators of an aircraft have rate, bandwidth, and magnitude constraints. When the control signal demanded by the backstepping controller cannot be generated by the actuators, that is, the actuators saturate, stability can no longer be guaranteed. The problem becomes worse

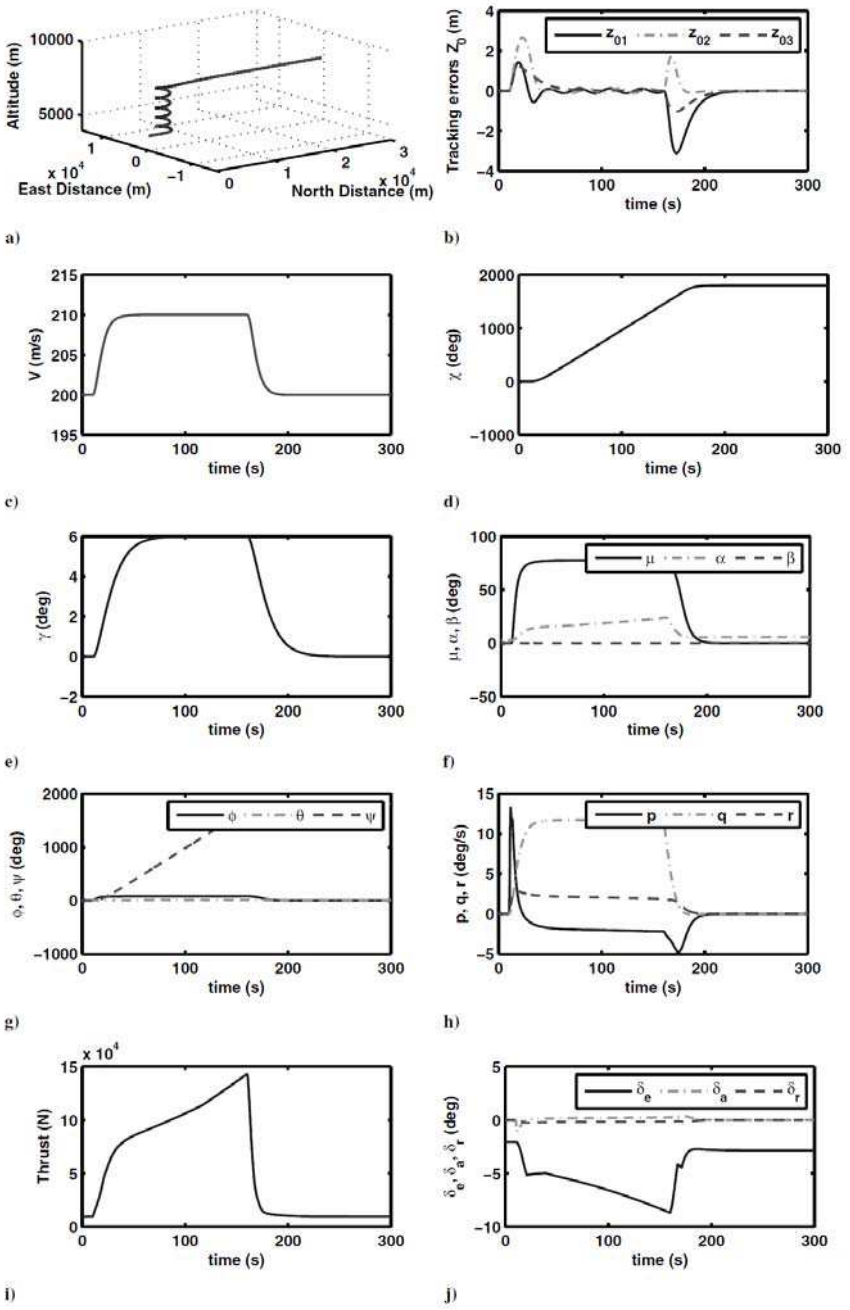

Fig. 3. Manoeuvre 1: climbing helical path performed at flight condition 1 without any uncertainty or actuator failures

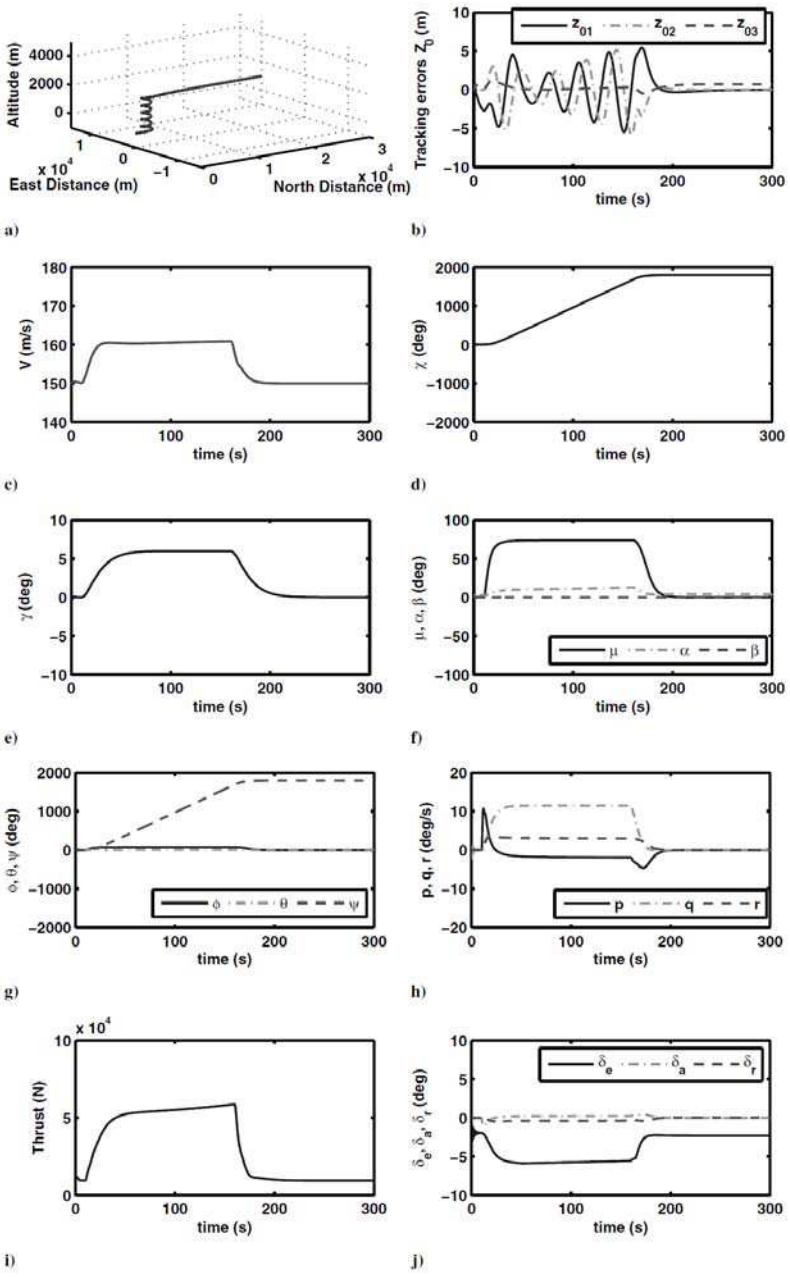

Fig. 4. Manoeuvre 1: climbing helical path performed at flight condition 2 with +30% uncertainties in the aerodynamic coefficients

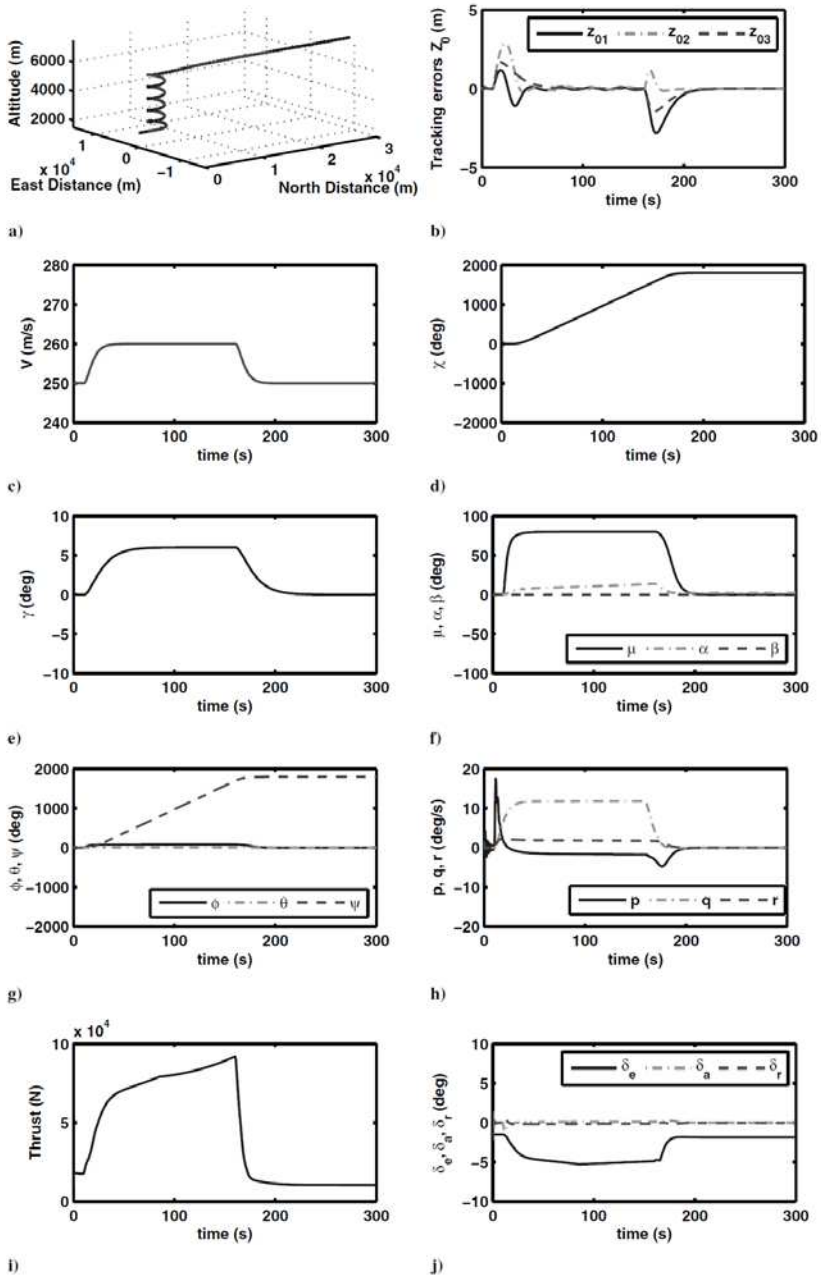

Fig. 5. Manoeuvre 1: climbing helical path performed at flight condition 3 with left aileron locked at -10 deg

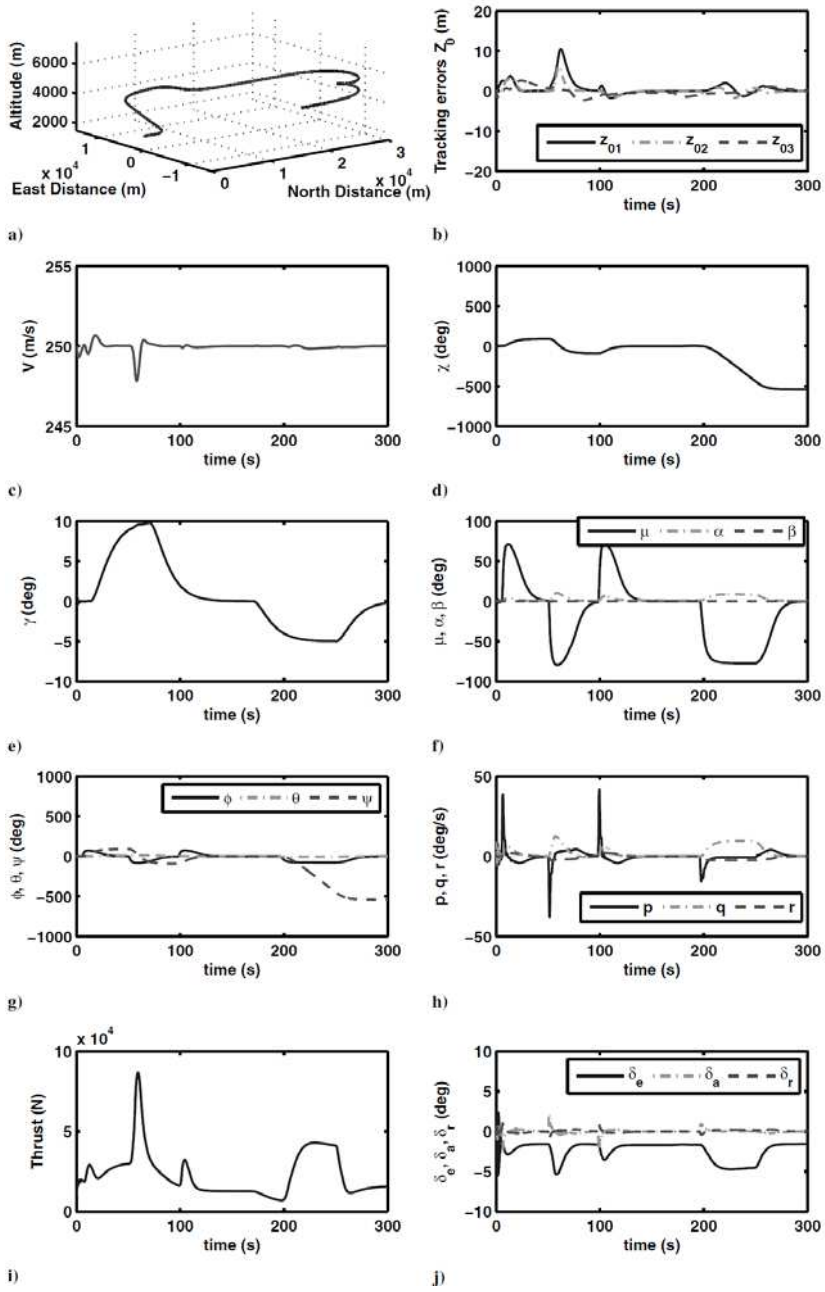

Fig. 6. Manoeuvre 2: reconnaissance and surveillance performance at flight condition 3 with -30% uncertainties in the aerodynamic coefficients

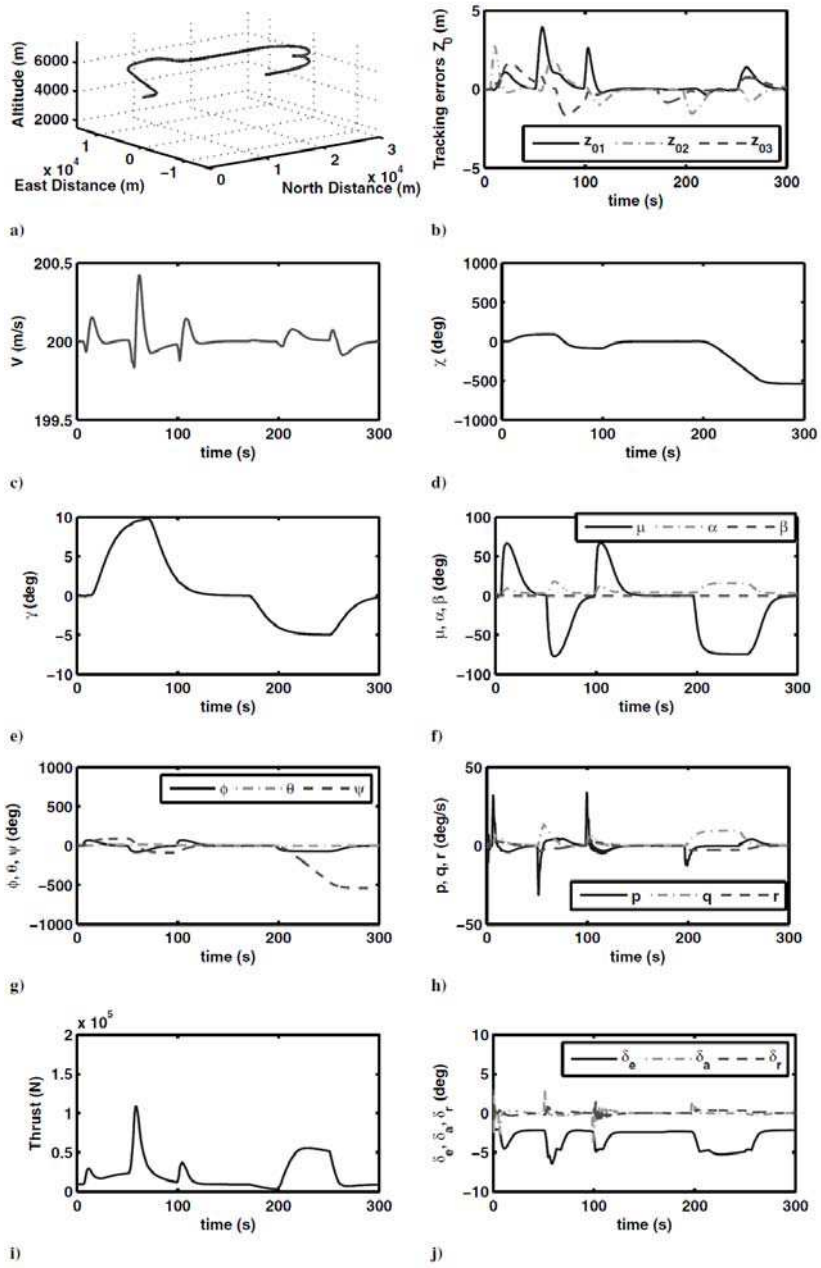

Fig. 7. Manoeuvre 2: reconnaissance and surveillance performance at flight condition 1 with left aileron locked at +10 deg.

when online parameter update laws are used, because these tend to be aggressive while seeking the desired tracking performance. Because the desired control signal is not achieved during saturation, the tracking error will increase. Because this tracking error is not just the result from the parameter estimation error, the update law may "unlearn" during these saturation periods.

In (Farrell et al., 2003, 2005) a method is proposed that fits within the recursive adaptive backstepping design procedure and deals with the constraints on both the control variables and the intermediate states used as virtual controls.An additional advantage of the method is that it also eliminates the two other drawbacks of the adaptive backstepping method, that is, the time consuming analytic computation of virtual control signal derivatives and the restriction to nonlinear systems of a lower-triangular form.

The proposed method extends the adaptive backstepping framework in two ways.

1. Command filters are used to eliminate the analytic computation of the time derivatives of the virtual controls. The command filters are designed as linear, stable, low-pass filters with unity gain from its input to its output. The inputs of these filters are the desired (virtual) control signals and the outputs are the actual (virtual) control signal and its time derivative. Using command filters to calculate the virtual control derivatives, it is still possible to prove stability in the sense of Lyapunov in the absence of constraints on the control input and state variables.

2. A stable parameter estimation process is ensured even when constraints on the control variables and states are in effect. During these periods the tracking error may increase because the desired control signal cannot be implemented due to these constraints imposed on the system. In this case the desired response is too aggressive for the system to be feasible and the primary goal is to maintain stability of the online function approximation. The command filters keep the control signal and the state variables within their mechanical constraints and operating limits, respectively. The effect these constraints have on the tracking errors can be estimated and this effect can be implemented in modified tracking error definitions. These modified tracking errors are only the result of parameter estimation errors as the effect of the constraints on the control input and state variables has been removed. These modified tracking errors can thus be used by the parameter update laws to ensure a stable estimation process.

The command filtered adaptive backstepping approach is summarized in the following theorem.

Theorem A.2 (Constrained Adaptive Backstepping Method): For the parameter strict-feedback system Eq. (15) the tracking errors are again defined as

$$z_i = x_i - y_r^{(i-1)} - \alpha_{i-1} \tag{A.19}$$

for $i = 1,2,\cdots,n$. The nominal or desired virtual control laws can be defined as

$$\alpha_i^0 = -c_i z - \overline{z}_{i-1} - \varphi_i^T \hat{\theta} + + \dot{\alpha}_{i-1} - \chi_{i+1}, \quad i = 1,2,\cdots,n-1 \tag{A20}$$

where

$$\overline{z}_{i-1} = z_i - \chi_i, \quad i = 1,2,\cdots,n \tag{A.21}$$

are the modified tracking errors and where

$$\dot{\chi}_i = -c_i \chi_i + \left(\alpha_i - \alpha_i^0\right), \quad i = 1,2,\cdots,n-1 \tag{A.22}$$

are the filtered versions of the effect of the state constraints on the tracking errors z_i. The nominal virtual control signals α_i^0 are filtered to produce the magnitude, rate, and bandwidth limited virtual control signals α_i and its derivatives $\dot{\alpha}_i$ that satisfy the limits imposed on the state variables. This command filter can for instance be chosen as (Farrell et al., 2005)

$$\begin{bmatrix} \dot{q}_1 \\ \dot{q}_2 \end{bmatrix} = \begin{bmatrix} q_2 \\ 2\zeta\omega_n \left[S_R\left(\frac{\omega_n^2}{2\zeta\omega_n} \left[S_M\left(\alpha_i^0\right) - q_1 \right] - q_2 \right) \right] \end{bmatrix}, \quad \begin{bmatrix} \alpha_i \\ \dot{\alpha}_i \end{bmatrix} = \begin{bmatrix} q_1 \\ q_2 \end{bmatrix} \tag{A.23}$$

where $S_M(\cdot)$ and $S_R(\cdot)$ represent the magnitude and rate limit functions, respectively. These saturation functions are defined similarly as

$$S_M(x) = \begin{cases} M & \text{if} \quad x \geq M \\ x & \text{if} \quad |x| < M \\ -M & \text{if} \quad x \leq -M \end{cases}$$

The effect of implementing the achievable virtual control signals instead of the desired ones is estimated by the χ_i filters. With these filters the modified tracking errors $\bar{z}_i$ can be defined. It can be seen from Eq. (A.21) that when the limitations on the states are not in effect the modified tracking error converges to the tracking error. The nominal control law is defined in a similar way as

$$u^0 = \frac{1}{\beta(x)}\left(-c_n z_n - \bar{z}_{n-1} - \varphi_n^T \hat{\theta} + \dot{\alpha}_{n-1} + y_r^{(n)} \right) \tag{A.24}$$

which is again filtered to generate the magnitude, rate, and bandwidth limited control signal u. The effect of implementing the limited control law instead of the desired one can again be estimated with

$$\dot{\chi}_n = -c_n \chi_n + \beta\left(u - u^0\right) \tag{A.25}$$

Finally, the update law that now uses the modified tracking errors is defined as

$$\dot{\hat{\theta}} = \Gamma \sum_{i=1}^{n} \varphi_i \bar{z}_i \tag{A.26}$$

The resulting control law will render the derivative of the control Lyapunov function

$$V = \frac{1}{2}\sum_{i=1}^{n} z_i^2 + \frac{1}{2}\tilde{\theta}^T \Gamma^{-1} \tilde{\theta} \tag{A.27}$$

negative definite, which means that the closed-loop system is asymptotically stable.

7. References

Clough, B. T. (2005), "Unmanned Aerial Vehicles: Autonomous Control Challenges, a Researchers Perspective," Journal of Aerospace Computing, Information, and Communication, Vol. 2, No. 8, pp. 327–347, doi: 10.2514/1.5588.

Wegener, S., Sullivan, D., Frank, J., and Enomoto, F. (2004), "UAV Autonomous Operations for Airborne Science Missions," AIAA 3rd "Unmanned Unlimited" Technical Conference, Workshop and Exhibit, AIAA Paper 2004-6416.

Papadales, B., and Downing, M. (2005), "UAV Science Missions: A Business Perspective," Infotech@Aerospace, AIAA Paper 2005-6922.

Tsach, S., Chemla, J., and Penn, D. (2003), "UAV Systems Development in IAI-Past, Present and Future," 2nd AIAA "Unmanned Unlimited" Systems, Technologies, and Operations-Aerospace Land, and Sea Conference, AIAA Paper 2003–6535.

Kaminer, I., Pascoal, A., Hallberg, E., and Silvestre, C. (1998), "Trajectory Tracking for Autonomous Vehicles: An Integrated Approach to Guidance and Control," Journal of Guidance, Control, and Dynamics, Vol. 21, No. 1, pp. 29–38, doi:10.2514/2.4229.

Boyle, D. P., and Chamitof, G. E. (1999), "Autonomous Maneuver Tracking for Self-Piloted Vehicles," Journal of Guidance, Control, and Dynamics, Vol. 22, No. 1, pp. 58–67, doi: 10.2514/2.4371.

Singh, S. N., Steinberg, M. L., and Page, A. B. (2003), "Nonlinear Adaptive and Sliding Mode Flight Path Control of F/A-18 Model," IEEE Transactions on Aerospace and Electronic Systems, Vol. 39, No. 4, pp. 1250–1262, doi: 10.1109/TAES.2003.1261125.

Ren, W., and Beard, R. W. (2004), "Trajectory Tracking for Unmanned Air Vehicles with Velocity and Heading Rate Constraints," IEEE Transactions on Control Systems Technology, Vol. 12, No. 5, pp. 706–716, doi:10.1109/TCST.2004.826956.

Ren, W., and Atkins, E. (2005), "Nonlinear Trajectory Tracking for Fixed Wing UAVs via Backstepping and Parameter Adaptation," AIAA Guidance, Navigation, and Control Conference and Exhibit, AIAA Paper 2005-6196.

No, T. S., Min, B. M., Stone, R. H., and K. C. Wong, J. E. (2005), "Control and Simulation of Arbitrary Flight Trajectory-Tracking," Control Engineering Practice, Vol. 13, No. 5, pp. 601–612, doi:10.1016/j.conengprac.2004.05.002.

Kaminer, I., Yakimenko, O., Dobrokhodov, V., Pascoal, A., Hovakimyan, N., Cao, C., Young, A., and Patel, V. (2007), "Coordinated Path Following for Time-Critical Missions of Multiple UAVs via L1 Adaptive Output Feedback Controllers," AIAA Guidance, Navigation, and Control Conference and Exhibit, AIAA Paper 2007-6409.

Pachter, M., D'Azzo, J. J., and J. L. Dargan (1994), "Automatic Formation Flight Control," Journal of Guidance, Control, and Dynamics, Vol. 17, No. 6, pp. 1380–1383.

Proud, A. W., Pachter, M., and D'Azzo, J. J. (1999), "Close Formation Flight Control,"AIAA Guidance, Navigation, and Control Conference, AIAA Paper 1999-4207.

Fujimori, A., Kurozumi, M., Nikiforuk, P. N., and Gupta, M. M. (2000), "Flight Control Design of an Automatic Landing Flight Experiment Vehicle," Journal of Guidance, Control, and Dynamics, Vol. 23, No. 2, pp. 373–376, doi:10.2514/2.4536.

Singh, S. N., Chandler, P., Schumacher, C., Banda, S., and Pachter, M. (2000), "Adaptive Feedback Linearizing Nonlinear Close Formation Control of UAVs," American Control Conference, Inst. of Electrical and Electronics Engineers, Piscataway, NJ, pp. 854–858.

Pachter, M., D'Azzo, J. J., and Proud, A. W. (2001), "Tight Formation Control," Journal of Guidance, Control, and Dynamics, Vol. 24, No. 2, pp. 246–254, doi:10.2514/2.4735.

Wang, J., Patel, V., Cao, C., Hovakimyan, N., and Lavretsky, E. (2008), "Novel L1 Adaptive Control Methodology for Aerial Refueling with Guaranteed Transient Performance," Journal of Guidance, Control, and Dynamics, Vol. 31, No. 1, pp. 182–193, doi:10.2514/1.31199.

Healy, A., and Liebard, D. (1993), "Multivariable Sliding Mode Control for Autonomous Diving and Steering of Unmanned Underwater Vehicles," IEEE Journal of Oceanic Engineering, Vol. 18, No. 3, pp. 327–339, doi:10.1109/JOE.1993.236372.

Narasimhan, M., Dong, H., Mittal, R., and Singh, S. N. (2006), "Optimal Yaw Regulation and Trajectory Control of Biorobotic AUV Using Mechanical Fins Based on CFD Parametrization," Journal of Fluids Engineering, Vol. 128, No. 4, pp. 687–698, doi:10.1115/1.2201634.

Kannelakopoulos, I., Kokotović, P. V., and Morse, A. S. (1991), "Systematic Design of Adaptive Controllers for Feedback Linearizable Systems," IEEE Transactions on Automatic Control, Vol. 36, No. 11, pp. 1241–1253, doi:10.1109/9.100933.

Krstić, M., Kanellakopoulos, I., and Kokotović, P. V. (1992), "Adaptive Nonlinear Control Without Overparametrization," Systems and Control Letters, Vol. 19, pp. 177–185, doi:10.1016/0167-6911(92)90111-5.

Singh, S. N., and Steinberg, M. (1996), "Adaptive Control of Feedback Linearizable Nonlinear Systems With Application to Flight Control," AIAA Guidance, Navigation, and Control Conference, AIAA Paper 1996-3771.

Härkegård, O. (2003), "Backstepping and Control Allocation with Applications to Flight Control," Ph.D. Thesis, Linköping Univ., Linköping, Sweden.

Farrell, J., Polycarpou, M., and Sharma, M. (2003), "Adaptive Backstepping with Magnitude, Rate, and Bandwidth Constraints: Aircraft Longitude Control," American Control Conference, American Control Conference Council, Evanston, IL, pp. 3898–3903.

Kim, S. H., Kim, Y. S., and Song, C. (2004), "A Robust Adaptive Nonlinear Control Approach to Missile Autopilot Design," Control Engineering Practice, Vol. 12, No. 2, pp. 149–154, doi:10.1016/S0967-0661(03)00016-9.

Shin, D. H., and Kim, Y. (2004), "Reconfigurable Flight Control System Design Using Adaptive Neural Networks," IEEE Transactions on Control Systems Technology, Vol. 12, No. 1, pp. 87–100, doi:10.1109/TCST.2003.821957.

Farrell, J., Sharma, M., and Polycarpou, M. (2005), "Backstepping Based Flight Control with Adaptive Function Approximation," Journal of Guidance, Control, and Dynamics, Vol. 28, No. 6, pp. 1089–1102, doi:10.2514/1.13030.

Sonneveldt, L., Chu, Q. P., and Mulder, J. A. (2006), "Constrained Adaptive Backstepping Flight Control: Application to a Nonlinear F-16/MATV Model," AIAA Guidance, Navigation, and Control Conference and Exhibit, AIAA Paper 2006-6413.

Sonneveldt, L., Chu, Q. P., and Mulder, J. A. (2007), "Nonlinear Flight Control Design Using Constrained Adaptive Backstepping," Journal of Guidance, Control, and Dynamics, Vol. 30, No. 2, pp. 322–336, doi:10.2514/1.25834.

Yip, P.-C. P. (1997), "Robust and Adaptive Nonlinear Control Using Dynamic Surface Controller with Applications to Intelligent Vehicle Highway Systems," Ph.D. Thesis, Univ. of California at Berkeley, Berkeley, CA.

Cheng, K. W. E., Wang, H., and Sutanto, D. (1999), "Adaptive B-Spline Network Control for Three-Phase PWM AC-DC Voltage Source Converter," IEEE 1999 International Conference on Power Electronics and Drive Systems, Inst. of Electrical and Electronics Engineers, Piscataway, NJ, pp. 467–472.

Ward, D. G., Sharma, M., Richards, N. D., and Mears, M. (2003), "Intelligent Control of Un-Manned Air Vehicles: Program Summary and Representative Results," 2nd AIAA Unmanned Unlimited Systems, Technologies and Operations Aerospace, Land and Sea, AIAA Paper 2003-6641.

Nguyen, L. T., Ogburn, M. E., Gilbert, W. P., Kibler, K. S., Brown, P. W., and Deal, P. L. (1979), "Simulator Study of Stall Post-Stall Characteristics of a Fighter Airplane with Relaxed Longitudinal Static Stability," NASA Langley Research Center, Hampton, VA.

Lewis, B. L., and Stevens, F. L. (1992), Aircraft Control and Simulation, Wiley, New York, pp. 1–54, 110–115.

Cook, M. V. (1997), Flight Dynamics Principles, Butterworth-Heinemann, London, pp. 11–29.

Swaroop, D., Gerdes, J. C., Yip, P. P., and Hedrick, J. K. (1997), "Dynamic Surface Control of Nonlinear Systems," Proceedings of the American Control Conference.

Kanayama, Y. J., Kimura, Y., Miyazaki, F., and Noguchi, T. (1990), "A Stable Tracking Control Method for an Autonomous Mobile Robot," IEEE International Conference on Robotics and Automation, Inst. of Electrical and Electronics Engineers, Piscataway, NJ, pp. 384–389.

Enns, D. F. (1998), "Control Allocation Approaches," AIAA Guidance, Navigation, and Control Conference and Exhibit, AIAA Paper 1998-4109.

Durham, W. C. (1993), "Constrained Control Allocation," Journal of Guidance, Control, and Dynamics, Vol. 16, No. 4, pp. 717–725, doi:10.2514/3.21072.

Ioannou, P. A., and Sun, J. (1995), Stable and Robust Adaptive Control, Prentice–Hall, Englewood Cliffs, NJ, pp. 555–575.

Babuška, R. (1998), Fuzzy Modeling for Control, Kluwer Academic, Norwell, MA, pp. 49–52.

Karason, S. P., and Annaswamy, A. M. (1994), "Adaptive Control in the Presence of Input Constraints," IEEE Transactions on Automatic Control, Vol. 39, No. 11, pp. 2325–2330, doi:10.1109/9.333787.

Krstić, M., Kokotović, P. V., and Kanellakopoulos, I. (1993), "Transient Performance Improvement with a New Class of Adaptive Controllers," Systems and Control Letters, Vol. 21, No. 6, pp. 451–461, doi:10.1016/0167-6911(93)90050-G.

Sonneveldt, L., van Oort, E. R., Chu, Q. P., and Mulder, J. A. (2007), "Comparison of Inverse Optimal and Tuning Functions Designs for Adaptive Missile Control," AIAA Guidance, Navigation, and Control Conference and Exhibit, AIAA Paper 2007-6675.

Page, A. B., and Steinberg, M. L. (1999), "Effects of Control Allocation Algorithms on a Nonlinear Adaptive Design," AIAA Guidance, Navigation, and Control Conference and Exhibit, AIAA, Reston, VA, pp. 1664–1674; also AIAA Paper 1999-4282.

Advances in Flight Control Systems

Edited by Dr. Agneta Balint

ISBN 978-953-307-218-0
Hard cover, 296 pages
Publisher InTech
Published online 11, April, 2011
Published in print edition April, 2011

Nonlinear problems in flight control have stimulated cooperation among engineers and scientists from a range of disciplines. Developments in computer technology allowed for numerical solutions of nonlinear control problems, while industrial recognition and applications of nonlinear mathematical models in solving technological problems is increasing. The aim of the book Advances in Flight Control Systems is to bring together reputable researchers from different countries in order to provide a comprehensive coverage of advanced and modern topics in flight control not yet reflected by other books. This product comprises 14 contributions submitted by 38 authors from 11 different countries and areas. It covers most of the currents main streams of flight control researches, ranging from adaptive flight control mechanism, fault tolerant flight control, acceleration based flight control, helicopter flight control, comparison of flight control systems and fundamentals. According to these themes the contributions are grouped in six categories, corresponding to six parts of the book.

INTECH
open science | open minds

InTech Europe
University Campus STeP Ri
Slavka Krautzeka 83/A
51000 Rijeka, Croatia
Phone: +385 (51) 770 447
Fax: +385 (51) 686 166
www.intechopen.com

InTech China
Unit 405, Office Block, Hotel Equatorial Shanghai
No.65, Yan An Road (West), Shanghai, 200040, China
中国上海市延安西路65号上海国际贵都大饭店办公楼405单元
Phone: +86-21-62489820
Fax: +86-21-62489821